SEEKING FURTHER KNOWLEDGE OF ROBO SIGNALING

WITH FORWARD GENETICS

by

Kendall A Rasband

A dissertation submitted to the faculty of
The University of Utah
in partial fulfillment of the requirements for the degree of

Doctor of Philosophy

Department of Neurobiology and Anatomy

The University of Utah

May 2011

The University of Utah Graduate School

STATEMENT OF DISSERTATION APPROVAL

The dissertation of **Kendall A Rasband**

has been approved by the following supervisory committee members:

Chi-Bin Chien	, Chair	**6/7/10** Date Approved
Richard L. Dorsky	, Member	**6/7/10** Date Approved
Edward Levine	, Member	**6/7/10** Date Approved
Sheryl Scott	, Member	**6/7/10** Date Approved
Monica Vetter	, Member	**6/7/10** Date Approved

and by **Monica Vetter**, Chair of the Department of **Neurobiology and Anatomy**

and by Charles A. Wight, Dean of The Graduate School.

ABSTRACT

How the nervous system generates its complex connectivity has intrigued scientists for over a century. The growing axons of developing neurons receive guidance information from their environment through receptors on the surface of their growth cones. The *roundabout* genes (or *robos*) represent one major receptor family, and Slits are their ligands. In Chapter 1, I summarize what is known about Slit-Robo signaling in both the *Drosophila* ventral nerve cord and the vertebrate visual system. I also review the molecules that are known to participate in Slit-Robo signaling.

Slits are generally thought to act as repellents for growth cones, and have been demonstrated biochemically to bind to Robo receptors. Although Slits are known to act through Robo receptors in *Drosophila*, this has not been formally tested in vertebrates. This distinction is important due to several differences between these two systems. In Chapter 2, I use an in vitro protocol that I have developed to culture zebrafish retinal ganglion cells (RGCs). Adding either human Slit2 (in conditioned media) or partially purified zebrafish Slit2 to these explant cultures confirms that Slit2 acts to collapse zebrafish RGCs. By performing similar collapse assays on explants that lack Robo2 receptor, I show that this Slit2 induced collapse of RGCs requires the Robo2 receptor.

The *astray* mutant (defective in the zebrafish homolog of Robo2) has provided much insight into Slit-Robo signaling in the vertebrate visual system. How this receptor transduces its signal to elicit changes in growth cone behavior is, however, poorly

understood. In Chapter 3, I present the results of a noncomplementation screen for *astray* that was designed to help understand Slit-Robo signaling. We screened 21,649 mutagenized haploid genomes and recovered 9 new alleles of *astray*. We sequenced these mutations and characterized their phenotypic strengths. Two new alleles of *astray* display a novel phenotype in which one or both optic tecta are innervated.

In Chapter 4, I discuss the results of the in vitro experiments and the new alleles from the screen. I also propose some future directions that could further expand our understanding of Slit-Robo signaling.

TABLE OF CONTENTS

LIST OF FIGURES

CHAPTER 1

INTRODUCTION

Overview

The question of how the brain develops is not a new one; scientists have been investigating this process for over a century. For the nervous system to function properly, neurons must establish the correct connectivity with appropriate partners. How receptors on the surface of growth cones sense cues in the environment and steer them properly is a main point of investigation for the field of axon guidance. Although many ligands and their receptors have been identified, how the signals ultimately lead to changes in growth cone dynamics is poorly understood. One of these pathways is the Slit-Robo signaling pathway. Slits are guidance cues, usually repulsive, which are detected by Robo receptors. In this first chapter, I will review what is known about the Slits and Robos, including other genes that have been shown to interact with them.

In vertebrates, Slits have not formally been shown to act through Robo receptors in guiding growth cones, although they are known to bind them. In the second chapter, I introduce a zebrafish retinal culture system and demonstrate 1) that Slits are repellent for developing zebrafish Retinal Ganglion Cells (RGCs) in culture, and 2) that this repellent activity is mediated by the Robo2 receptor. Recent experimental evidence from our laboratory (Hardy and Chien, unpublished results) suggests that Slit1a is not functioning as a simple repellent in the zebrafish visual system. Therefore, I attempted to test Slit1a's function in culture, although ultimately I was unable to do so due to technical difficulties.

Though they were first characterized in *Drosophila*, Slits and Robos have been found in other animals from *C. elegans* to chick, *Xenopus*, mouse, and human. Although some molecules that interact with Robo have been found in different systems, we cannot

yet draw a comprehensive signaling pathway. In the third chapter, I describe a genetic screen that I performed to isolate mutant alleles that could help us to better understand Slit-Robo signaling.

Finally, in the last chapter, I discuss both the results of the culture experiments and the genetic screen, as well as some future directions in which the work could continue.

Axon Pathfinding Overview

Much of the complex structure of the vertebrate brain is determined by guidance decisions of developing growth cones. These growth cones express various receptors on their surface that sense spatial information. Considered simply, this information can be either positive or negative. For example, positive signals are important in attracting axons to their exit point in the eye, and then negative signals act repulsively to prevent axons from straying from the proper path as they cross the optic chiasm to the other side of the brain. These negative signals may not only inhibit improper growth, but cause straying axons to retract until they return to the proper pathway.

Small differences in expression levels of cues can be detected between opposite sides of the growth cone, leading to changes in direction. These changes are driven by spatial rearrangements of actin and microtubule networks in the growth cone. For example, Netrins are a class of guidance signal that usually act positively. If a growth cone is progressing through an area that presents a higher concentration of Netrin on its left side, this side would have its cytoskeletal networks stabilized, and growth would increase on that side, resulting in a leftward turn.

Generating the enormous variety of connections found in the vertebrate brain requires complex growth cone responses. These can be achieved in several ways. Different growth cones express different components of receptors, and regulate receptor levels over time. Individual growth cones can switch their response to a given signal between one point in their pathway and another. Growth cones can express different downstream signal transduction components and so respond differently. Understanding how these receptors and ligands transduce a signal to affect axon guidance is the goal of 1) the in vitro experiments of Chapter 2 and 2) the forward genetic screen of Chapter 3.

Axon Guidance in the Zebrafish Visual System

Zebrafish as a Model Genetic System

Several features of the zebrafish, *Danio rerio*, make it a good system for studying axon guidance. The fish are relatively small and easy to both maintain and breed. They have external fertilization and the transparency of their larvae allows excellent visualization of the visual pathway. A breeding pair can produce over a hundred offspring from a single mating; and matings can be repeated every week.

General tools such as in situ hybridization and mutagenesis are well established in zebrafish. In addition, specific transgenic lines exist that allow labeling of the visual pathway in live animals. A large-scale screen was conducted in Tübingen, Germany, over a decade ago that resulted in numerous mutants including more than 20 with defects in retinal pathfinding (Baier et al., 1996; Haffter et al., 1996; Karlstrom et al., 1996; Trowe

et al., 1996). This screen demonstrated the usefulness of zebrafish as a genetic system, with particular emphasis on early developmental processes.

Retinotectal System in Zebrafish

The visual pathway is well characterized in vertebrates, including zebrafish (Stuermer, 1988; Wilson et al., 1990; Burrill and Easter, 1995). The first RGCs are born in the eye at about 28 hours post fertilization (hpf). The first pioneer axons exit the eye at the optic nerve head at 30 hpf. These axons continue toward the midline, forming the optic chiasm together with the axons from the contralateral eye at 32 hpf. After passing through the chiasm, the axons continue laterally and then turn dorsally and caudally as they enter the optic tract at 36 hpf. The first pioneer axons eventually reach the optic tectum, their primary target, at 48 hpf.

Zebrafish do not have binocular vision, and so all the retinal axons cross to the contralateral side, in contrast to other vertebrates that often have a subset that project ipsilaterally at the chiasm. Developing axons maintain topography along both the antero-posterior and dorso-ventral axes as they navigate from the eye to the tectum (Steurmer, 1988).

Many retinal pathfinding mutants now exist in zebrafish, most of which were generated from the large-scale Tübingen screen (Trowe et al., 1996; Karlstrom et al., 1996). These mutants make various types of pathfinding mistakes throughout the entire course of the retinal pathway including defects in exiting the eye, crossing at the midline, tract sorting and topography, and pathfinding to the tectum (Hutson and Chien, 2002b). One of these mutants was *astray*, which makes pathfinding errors throughout the

pathway. Cloning of *astray* (Fricke et al., 2001) showed it to be defective in zebrafish Robo2, a homolog of the *Drosophila* Roundabout receptor.

Drosophila Slit-Robo Signaling

The Repulsive Ligand Slit

Slit and its receptor, Roundabout (or Robo), define one of the major canonical axon guidance pathways. Both genes were first characterized in the *Drosophila* ventral nerve cord. In this system, there are two longitudinal tracts that run parallel to and on either side of the midline. The axons comprising these tracts can be divided into two types: the 10% that never cross the midline and the 90% that cross the midline exactly once (Kidd et al., 1998a). The crossing axons form commissures, giving the overall system a ladder-like structure.

In the *slit* mutant, the absence of this repellent protein results in all axons in the ventral nerve cord collapsing onto the midline (Kidd et al., 1999). Later studies showed that Slit is expressed in a band at the midline, being secreted by midline glial cells. It acts as a repellent, keeping longitudinal axons out of the midline, even though attractive guidance cues such as Netrin are present there (Kidd et al., 1999).

Slit was cloned and found to be a large, extracellularly secreted protein with several domains implicated in protein-protein interactions (Rothberg et al., 1988; Rothberg et al., 1990). It is unusual in that it contains both Epidermal Growth Factor (EGF) and Leucine Rich Repeat (LRR) domains (Figure 1.1). More commonly, a protein will contain only EGF or LRR domains, but not both. These domains are important for

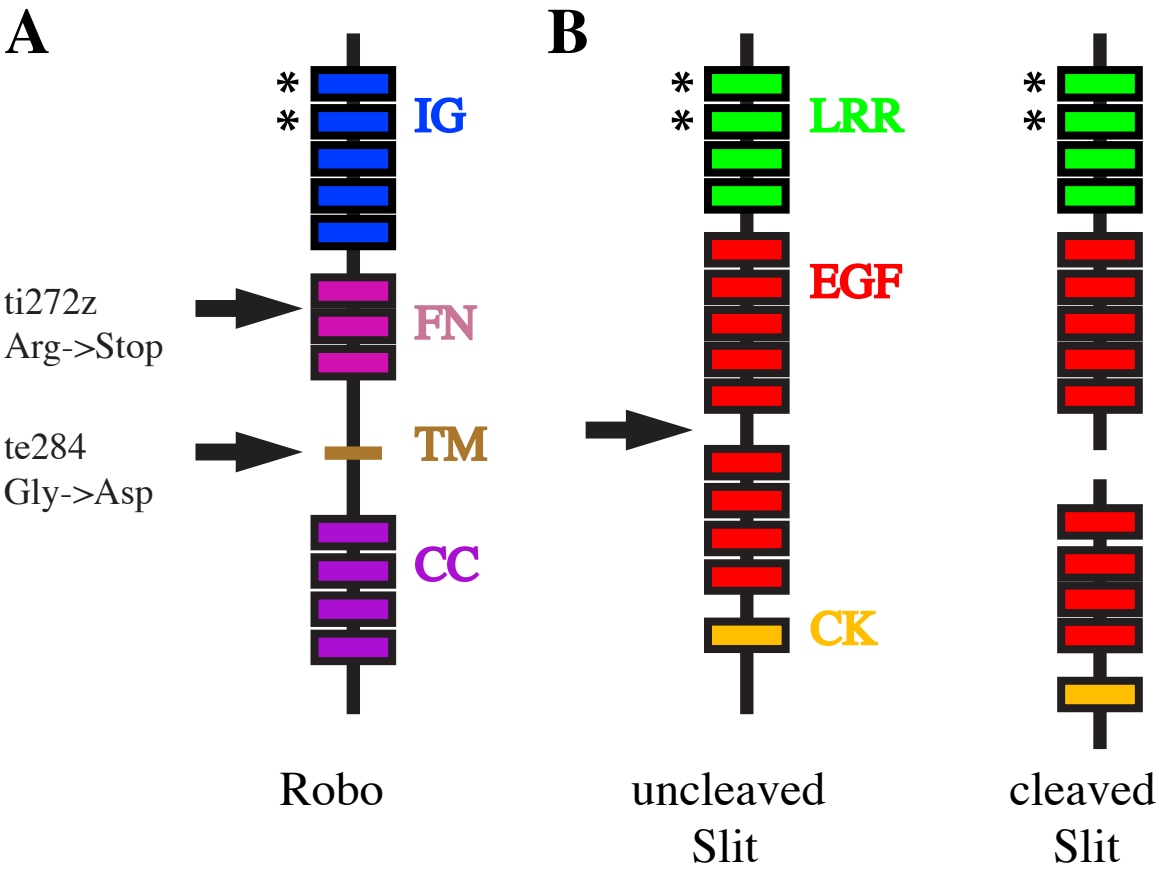

Figure 1.1 Robo and Slit Structure. (A) The domain structure of a generalized Robo receptor including: Immunogloblulin (IG), Fibronectin (FN), Transmembrane (TM), and Conserved Cytoplasmic (CC) domains. The arrows show the location of the mutations of the ti272z and te284 alleles of zebrafish astray (robo2). (B) Generalized structure and cleavage of Slit proteins including Leucine Rich Repeats (LRRs), Epidermal Growth Factor (EGF) and Cysteine Knot (CK) domains. The arrow shows the site where Slit is cleaved into 140kD and 55kD fragments. The asterisks show the domains required for Robo-Slit binding.

protein-protein interactions, and the presence of multiple domains suggests that Slit interacts with several other proteins.

Robos, the Receptors for Slits

Robo was first isolated in *Drosophila* in a screen designed to identify mutations in genes important for determining CNS pathways (Seeger et al., 1993). In *robo* mutants, axons cross and recross the midline several times, so that the CNS resembles a series of traffic roundabouts, giving the mutant its name. Cloning of the Robo receptor showed that it defines a novel subfamily of the immunoglobulin superfamily. Robo has five immunoglobulin (IG) and three fibronectin (FN) domains in its extracellular domain (Figure 1.1). Consistent with its role as a receptor, it also has a single transmembrane (TM) domain and a long cytoplasmic domain (Kidd et al., 1998b). The cytoplasmic domain contains several conserved cytoplasmic (CC) motifs that are either proline-rich or bear tyrosines, and so were considered good candidates for protein interactions.

Slit has been shown to be the repulsive ligand for the Robo receptor (Kidd et al., 1999). The mutant phenotype of *robo* is weaker than *slit*, although both result in axons spending more time at the midline than in wildtype. This suggested the possibility of one or more additional Slit receptors. Three Robo genes are now known in *Drosophila*. A gain-of-function screen identified the gene for the Robo2 receptor (Rajagopalan et al., 2000a), and a subsequent *robo2* loss-of-function mutant was created by imprecise P-element excision. A *robo3* mutant was found serendipitously from an unrelated screen (Rajagopalan et al., 2000b). Both of these receptors have a similar structure to Robo, except that they lacked some of the CC domains (Kidd et al., 1998b; Bashaw et al.,

2000). Like the *robo* mutant, *robo2* and *robo3* single mutants demonstrated a weaker phenotype than *slit*. It was found that removing additional copies of *robo* genes, for instance in *robo; robo2* double mutants, yielded very similar phenotypes to *slit* mutants (Simpson et al., 2000b). Simply put, any single *robo* mutant has a phenotype weaker than *slit*, but if any two or all three of the Robo receptors are removed, the phenotype resembles that of *slit* (Simpson et al., 2000b; Rajagopalan et al., 2000b).

Robo receptors are expressed at high levels on noncrossing axons from the outset, preventing them from crossing the midline. Axons that do cross the midline do not express Robo until after they cross (Simpson et al., 2000a; Kidd et al., 1998a). The upregulation of Robo after crossing prevents any subsequent midline crossings.

The expression pattern of multiple Robo family receptors led to a "combinatorial code" hypothesis in which increasing the number of receptor genes expressed on a growth cone moves it further laterally away from the repulsive Slit at the midline. This is consistent with the loss of function analysis in which removing additional Robo genes leads to a more severe phenotype. Also, overexpressing these genes leads to the shifting of longitudinal axons away from the midline (Kidd et al., 1998a, Rajagopalan et al., 2000a).

Slits have been shown to bind Robos in vitro (Brose et al., 1999; Simpson et al., 2000b) and a crystal structure is now known (Howitt et al., 2004). The first two IG domains of Robo are important for binding Slit (Liu et al., 2004); the first and second LRR domains of Slit are important for binding to Robos (Battye et al., 2001) but the function of the EGF domains remains unknown. This is consistent with the observation

that generally the N-terminal portion of cleaved Slit has the same biological function as full-length Slit (Nguyen Ba-Charvet et al., 2001; Chen et al., 2001).

Commissureless Acts as a Gate Keeper by Regulating Robos

An important question is how Robo is downregulated on commissural axons to allow them to cross the midline. The *commissureless* (*comm*) gene was identified in the same screen for CNS mutants that found *robo* (Seeger et al., 1993). *comm* mutants have a striking phenotype: they completely lack commissures, leaving only the longitudinal axon pathways (Tear et al., 1996). This is the opposite of the phenotype seen in *slit* or multiple *robo* mutants in that rather than spending additional time at the midline, axons avoid the midline altogether. Comm is a small protein with a single transmembrane domain that antagonizes Robo signaling and allows axons to cross the midline (Tear et al., 1996), functioning in a dosage-sensitive and complementary manner with Robo (Kidd et al., 1998a). Comm downregulates Robo function by redirecting Robo from the synthetic pathway to an endocytic pathway (Keleman et al., 2002). After a growth cone crosses the midline, *comm* expression is turned off, allowing the expression of Robos on the cell surface to prevent any recrossing of the midline. Increasing the level of Comm decreases the levels of all Robo family members (Rajagopalan et al., 2000a).

Slit-Robo Signaling in the Zebrafish Visual System

astray, the Zebrafish Homolog of *robo2*

There are four Robo genes in vertebrates (*robo1-4*). In the zebrafish visual pathway, only Robo2 is expressed by RGCs (Lee et al., 2001; Campbell et al., 2007). The large-scale Tübingen screen (Karlstrom et al., 1996) identified mutants in the gene *astray*, the zebrafish *robo2*. These mutants make mistakes throughout the visual pathway, with retinal axons often entering regions of Slit expression. Whole eye transplants demonstrated that *astray* acts eye autonomously (Fricke et al., 2001). There were originally four alleles of *astray* identified: *te284, ti272z, te378,* and *tl231*; all are fully penetrant and recessive. Two alleles were characterized molecularly (Fricke et al., 2001). *ti272z*, the best characterized of the alleles, encodes an early stop codon before the TM domain, rendering Robo2 unable to function as a receptor. *te284* encodes a missense mutation within the TM domain. The *te284* allele has a noticeably weaker phenotype than the other three alleles (which were all considered to have roughly equal strong phenotypes), making retinal pathfinding mistakes that are on average less severe. Chapter 2 characterizes *ti272z* and *te284* function in culture, while Chapter 3 isolates and characterizes nine new alleles of *astray*.

Slit Structure and Function in Vertebrates

Although there is only one *slit* gene in invertebrates, there are three (*slit1-3*) in mammals and four (*slit1a, slit1b, slit2* and *slit3*) in fish (Itoh et al., 1998). Teleost *slit1* has undergone a gene duplication event, yielding *slit1a* and *slit1b* in zebrafish (Hutson et

al., 2003). At the optic chiasm, Slits are expressed in overlapping patterns consistent with their functioning as repellents to keep axons from wandering off the proper pathway. Here, the combined expression of zebrafish Slit2 and Slit3 (Figure 1.2) is analogous to the combined expression of Slit1 and Slit2 in the mouse (Rasband et al., 2003)

Both vertebrate Slit1 and Slit2 are known to be proteolytically cleaved, but it is likely that all Slits are cleaved (Wang et al., 1999; Whitford et al., 2002). In the experiments that have tested the cleavage products' function, it is either full-length Slit or the large N-terminal fragment that have biological activity, while the smaller C-terminal portion is not known to have any function (Nguyen Ba-Charvet et al., 2001; Chen et al., 2001).

In the mouse visual system, *slit* mutants do not have a strong phenotype unless multiple *slit* genes are removed (Plump et al., 2002). This is consistent with their overlapping expression patterns at the optic chiasm. The presence of Slits surrounding the visual pathway together with the repellent nature of Slits led to the 'guardrail hypothesis' in which Slits are thought to act to set boundaries for developing axons (Hutson and Chien, 2002a). There are no known *slit* mutants in the zebrafish.

Slit In Vitro Experiments

Several in vitro experiments have been done to assay the function of Slits directly. Growth cones from mouse RGCs (Erskine et al., 2000), rat diencephalon (Ringstedt et al., 2000), and chick RGCs (Niclou et al., 2000), either collapse or are repelled by the presence of Slit2 in culture. Additionally, RGC growth cones derived from different quadrants of the chick retina do not show any difference in their response to Slit2. In

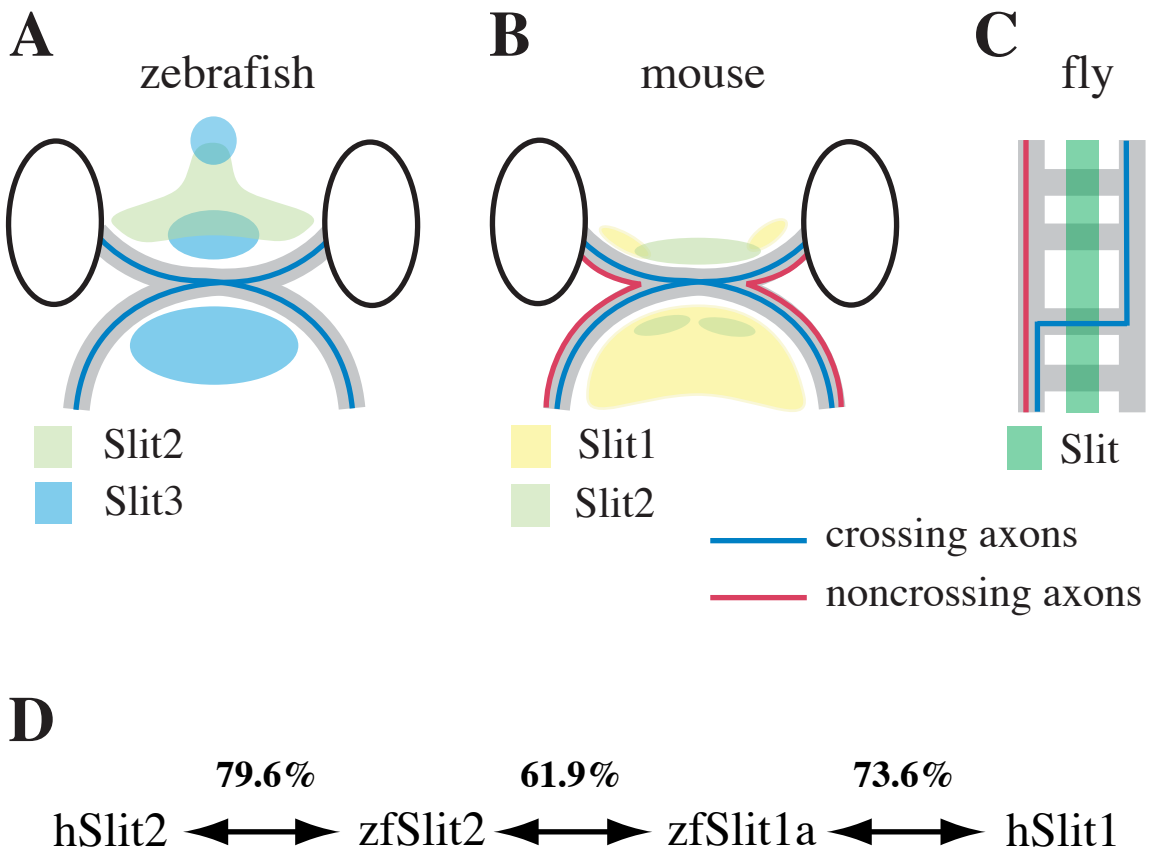

Figure 1.2 Slit Expression and Conservation. (A) The expression pattern of zebrafish Slit2 and Slit3 at the optic chiasm, consistent with their functioning as 'guardrails' at the midline. (B) The expression pattern of Slit1 and Slit2 at the mouse optic chiasm. Combined mouse Slit1 and Slit2 expression is similar to the combined zebrafish Slit2 and Slit3 expression patterns (adapted from Rasband et al., 2003). (C) The ventral nerve cord in Drosophila showing Slit expression in a stripe at the midline. Crossing axons are shown in blue and noncrossing axons in red. (D) Figure showing the % similarity between some Slit family members.

mouse, both Slit1 and Slit2 inhibit growth of mouse RGC axons in culture (Plump et al., 2002). These results are consistent with the 'guardrail model' of combined Slits acting as repellents at the midline.

Slits are generally thought of as having a negative or repellent nature, especially at the midline. However, in vitro they have also been reported to increase branching in cortical dendrites (Whitford et al., 2002) and in sensory axons (Wang et al., 1999). Strictly speaking, branching is distinct from repulsion or attraction, but these results mean that it is likely that Slit function is more complex than always being a repellent.

Signaling Differences Between *Drosophila* and Vertebrates

Although there are similarities between Slit-Robo signaling in the *Drosophila* ventral nerve cord and the vertebrate optic chiasm, there are also several key differences. In *Drosophila*, there is one *slit* gene and multiple *robo* genes. In the vertebrate visual system, this situation is reversed, with one *robo* and multiple *slits*. An additional potential difference is the function of zebrafish Slit1a, which according to in vivo data from our laboratory, may act substantially differently from other Slits. Slit1a is expressed broadly in the forebrain, so that retinal axons grow directly over Slit1a-expressing domains (Hardy and Chien, unpublished data). This expression pattern suggests that it does not act as a repulsive cue. Also, both overexpression and morpholino experiments suggest that Slit1a is not acting as a simple repellent (Hardy and Chien, unpublished data).

Another difference is in the arrangement of commissures in the two systems. In the fly ventral nerve cord, many axons cross only once, while others never cross. This midline crossing is permitted by the presence of Comm, a protein that inhibits Robo

expression until after the axons have crossed the midline (Kidd et al., 1998a). In this system, Slit acts as a gatekeeper, only allowing axons to cross after Robo is downregulated by Comm. In the vertebrate visual system, axons do not ever cross a region of Slit expression near the midline. Instead, Slits seem to be functioning as guardrails to keep axons on the proper path. Therefore, Robo function need not be downregulated, consistent with the lack of a known *comm* gene in vertebrates.

There are also some differences in structure between Robo family members in fly. *Drosophila* Robo2 and Robo3 do not have a CC2 or CC3 domain (Bashaw et al., 2000). Across all Robos (both fly and vertebrates), the extracellular portion of the receptor is much more highly conserved than the intracellular region (Simpson et al., 2000b).

Slit-Robo Signaling Pathway

In both *Drosophila* and vertebrates, Slit and Robo possess several domains that have been implicated in protein interactions. Several molecules have been identified as interacting along this signaling pathway and some of them are known to interact with particular domains of the receptor or ligand. These interactions with the Slit-Robo signaling pathway are summarized in Figure 1.3.

Abelson and Enabled

Abelson (Abl) and its substrate Enabled (Ena) have both been shown to bind directly to the cytoplasmic region of Robo. Abl is a tyrosine kinase that antagonizes Robo signaling, whereas Ena is required for proper Robo signaling (Bashaw et al., 2000). Abl can also form a complex with Robo and N-cadherin that results in local loss of N-

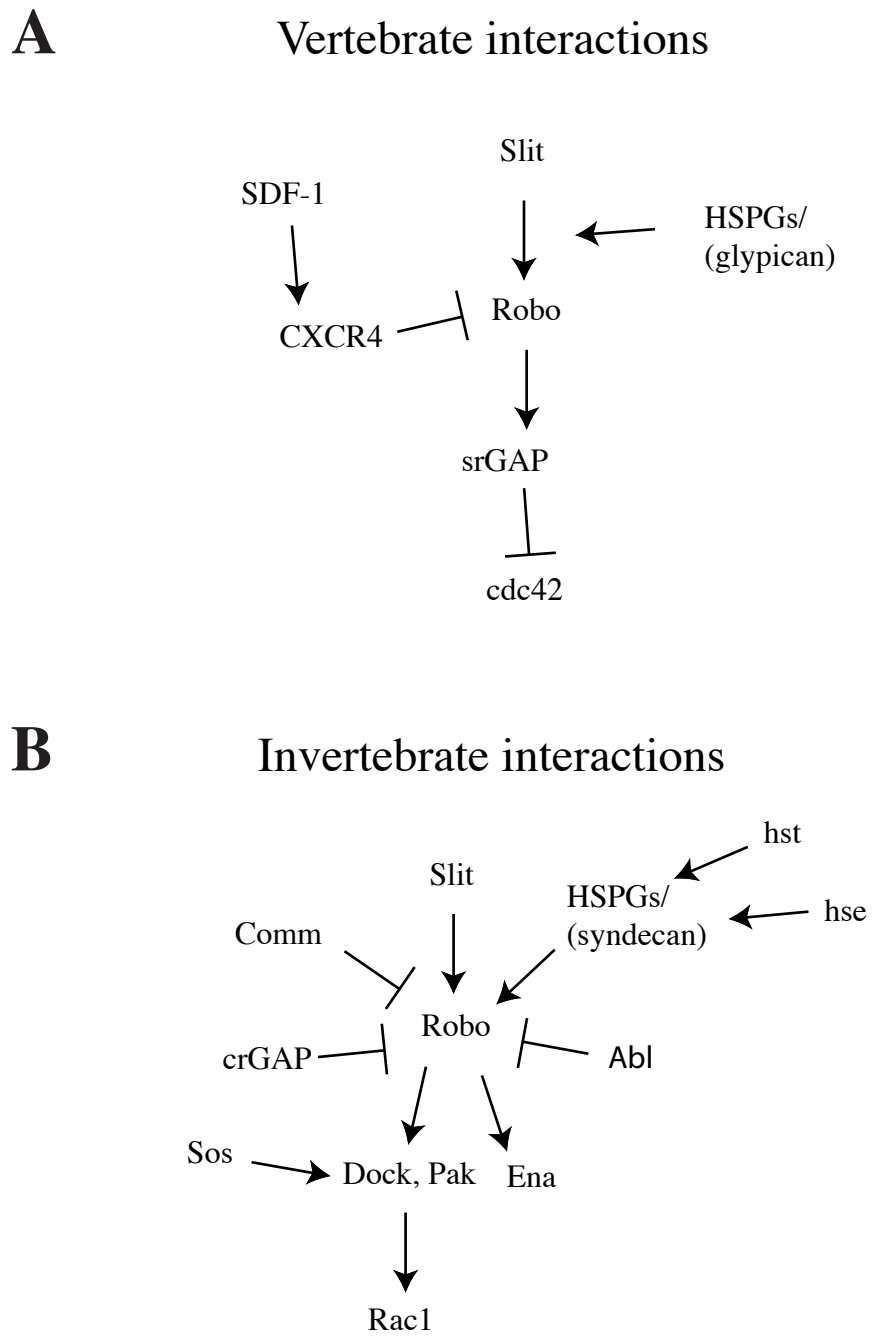

Figure 1.3 Robo Signaling Interactions. (A) A summary of known vertebrate interactions. SDF-1 and CXCR4 are a chemokine and its receptor, respectively. Robo is known to interact through Slit-Robo GAPs (srGAPs) to inhibit cdc42. (B) Summary of known invertebrate interactions. crossGAP (crGAP) inhibits Robo signaling. Slit binding enhances formation of a complex of Robo with Dock and Pak. Son of sevenless (Sos) forms a complex with Dock and Robo that signals to Rac. Commisureless (Comm) and Abelson (Abl) inhibit Robo signaling. Robo signaling acts through Enabled (Ena).

cadherin-mediated adhesion (Rhee et al., 2002). This is thought to be a mechanism that allows for turning by promoting growth and attachment on one side of the growth cone and repressing it on the other.

Slit-Robo Signaling Acts Through Dock and Pak

Dreadlocks (Dock) and p21-activated serine-threonine kinase (Pak) have both been shown to interact with Robo signaling. In *Drosophila*, Dock has been shown to directly bind to the cytoplasmic domain of Robo and this binding is enhanced by Slit, which helps to form a complex with Dock and Pak, increasing Rac1 activity. Loss-of-function mutations in Dock, Pak, or Rac1 result in a reduction of Robo signaling (Fan et al., 2003).

GTPase Activating Proteins

Rac and Rho are two small GTPases that are regulated by Guanine Exchange Factors (GEFs) and GTPase Activating Proteins (GAPs). GAPs have been shown to have a function in axon pathfinding and may provide a means of linking the Robo signaling pathway with changes in the cytoskeleton. In *Drosophila*, *crossGAP*, or *crGAP*, also known as *vilse* (Hu et al., 2005), binds to the second intracellular CC domain of Robo and *crGAP* mutants are similar to *robo* mutants (Lundstrom et al., 2004). This represents an apparent inconsistency in the literature in that overexpression and RNAi experiments show that *crGAP* acts to antagonize Robo signaling (Hu et al., 2001).

Another class of GAPs, the vertebrate Slit-Robo GAPs (srGAPs), were isolated from a yeast two-hybrid screen (Wong et al., 2001). The srGAPs have been shown to

bind to the CC2 and CC3 domains of Robo1 (Wong et al., 2001, Li et al., 2006). The srGAPs do not have representative members in *C. elegans* or *Drosophila*. Robo signaling promotes srGAP activity which then inactivates cdc42. On the other hand, crGAP seems to be down-regulated by Robo signaling.

Son of sevenless (Sos), a GEF that regulates both Ras and Rho, forms a complex with Robo and Dock that regulates cytoskeletal rearrangement. Although Sos can regulate several GTPases, this rearrangement of the cytoskeleton is dependent on Rac, but not Ras (Yang and Bashaw, 2006).

HSPGs

Heparan sulfate proteoglycans (HSPGs) were shown to have an important role in axon guidance when it was observed that mutants in EXT1, an HS polymerizing gene, have guidance defects in the mouse (Inatani et al., 2003). They function by promoting the binding of Slit to the Robo receptor, and removal of heparan sulfate impairs the effect of Slit (Hu et al., 2001). Glypicans and syndecans are two families of HSPG core proteins. Syndecan mutants exist for both *C. elegans* (Rhiner et al., 2005) and *Drosophila* (Steigeman et al., 2004), and both have been shown to interact with Slit-Robo signaling. In vertebrates, Glypican-1 interacts with either the full-length or C-terminal fragment of Slit2, but only very weakly with the N-terminal piece (Ronca et al., 2001). Heparin has been shown to bind the Slit-Robo complex in vitro (Hu et al., 2001), and crystal structures show that it is the first and second IG domain of Robo and the second LRR domain of Slit that form a complex with heparin (Hussain et al., 2006; Fukuhara et al., 2008).

In *C. elegans*, heparan sulfate-modifying enzymes such as *hse* and *hst* have been shown to genetically interact on the Slit pathway (Bulow et al., 2004). In zebrafish, HSPGs are required for proper axon sorting in the optic tract. *boxer* (a zebrafish homolog of *extl3*) and *dackel* (a zebrafish homolog of *ext2*) are mutants for two glycosyltransferase genes that are required for proper HS synthesis (Lee et al., 2004). Interestingly, *dak;box* double mutants phenocopy some of the *astray* pathfinding errors suggesting that Robo signaling requires HSPGs.

SDF-1 and CXCR4

In vertebrates, the SDF-1/CXCR4 pathway has been linked to Slit-Robo signaling. Both SDF-1 and CXCR4 are expressed in the chick retina (Chalasani et al., 2003a). Although it does promote cell survival through its receptor, CXCR4, the chemokine SDF-1 has by itself no effect on RGC axon pathfinding. However, SDF-1 does act to reduce the repellent activity of Slit2 in chick RGCs (Chalasani et al., 2003b). In zebrafish, morpholinos to SDF-1 or CXCR4 can partially rescue the retinal axon phenotype of the hypomorphic *astray* ^{te284} mutants, but not null *astray* ^{ti272z} mutants (Chalasani et al., 2007). In *astray* ^{ti272z}, the lack of any functional receptor means there is absolutely no Robo signaling. Although Robo signaling is reduced in *astray* ^{te284} mutants, it is still present at some level so that SDF-1 can modulate the signal's effects.

Conclusions

The identification of the Robo receptors as one of the main canonical families of axon guidance receptors has led to the identification of some molecules important for this

signaling pathway. Most of what we do know about Slit-Robo signaling comes from work in *Drosophila* and it is not clear what differences will exist compared to vertebrates. For example, it has never been formally shown that Slits are ligands for Robos in a vertebrate. I address this with the in vitro experiments of Chapter 2. A large-scale screen in zebrafish identified several mutants in retinal pathfinding, including *astray*, the homolog of the Robo2 receptor. However, the lack of mutants in genes that interact with Robo2 has limited our ability to learn more about Slit-Robo signaling. In Chapter 3, I discuss a screen designed to help us learn more about this signaling pathway.

References

Baier, H., S. Klostermann, T. Trowe, R. O. Karlstrom, C. Nusslein-Volhard and F. Bonhoeffer (1996). "Genetic dissection of the retinotectal projection." Development 123: 415-25.

Bashaw, G. J., T. Kidd, D. Murray, T. Pawson and C. S. Goodman (2000). "Repulsive axon guidance: Abelson and Enabled play opposing roles downstream of the roundabout receptor." Cell 101(7): 703-15.

Battye, R., A. Stevens, R. L. Perry and J. R. Jacobs (2001). "Repellent signaling by Slit requires the leucine-rich repeats." J Neurosci 21(12): 4290-8.

Brose, K., K. S. Bland, K. H. Wang, D. Arnott, W. Henzel, C. S. Goodman, M. Tessier-Lavigne and T. Kidd (1999). "Slit proteins bind Robo receptors and have an evolutionarily conserved role in repulsive axon guidance." Cell 96(6): 795-806.

Bulow, H. E. and O. Hobert (2004). "Differential sulfations and epimerization define heparan sulfate specificity in nervous system development." Neuron 41(5): 723-36.

Burrill, J. D. and S. S. Easter, Jr. (1995). "The first retinal axons and their microenvironment in zebrafish: cryptic pioneers and the pretract." J Neurosci 15(4): 2935-47.

Campbell, D. S., S. A. Stringham, A. Timm, T. Xiao, M. Y. Law, H. Baier, M. L. Nonet and C. B. Chien (2007). "Slit1a inhibits retinal ganglion cell arborization and synaptogenesis via Robo2-dependent and -independent pathways." Neuron 55(2): 231-45.

Chalasani, S. H., F. Baribaud, C. M. Coughlan, M. J. Sunshine, V. M. Lee, R. W. Doms, D. R. Littman and J. A. Raper (2003a). "The chemokine stromal cell-derived factor-1 promotes the survival of embryonic retinal ganglion cells." J Neurosci 23(11): 4601-12.

Chalasani, S. H., K. A. Sabelko, M. J. Sunshine, D. R. Littman and J. A. Raper (2003b). "A chemokine, SDF-1, reduces the effectiveness of multiple axonal repellents and is required for normal axon pathfinding." J Neurosci 23(4): 1360-71.

Chalasani, S. H., A. Sabol, H. Xu, M. A. Gyda, K. Rasband, M. Granato, C. B. Chien and J. A. Raper (2007). "Stromal cell-derived factor-1 antagonizes slit/robo signaling in vivo." J Neurosci 27(5): 973-80.

Chen, J. H., L. Wen, S. Dupuis, J. Y. Wu and Y. Rao (2001). "The N-terminal leucine-rich regions in Slit are sufficient to repel olfactory bulb axons and subventricular zone neurons." J Neurosci 21(5): 1548-56.

Erskine, L., S. E. Williams, K. Brose, T. Kidd, R. A. Rachel, C. S. Goodman, M. Tessier-Lavigne and C. A. Mason (2000). "Retinal ganglion cell axon guidance in the mouse optic chiasm: expression and function of robos and slits." J Neurosci 20(13): 4975-82.

Fan, X., J. P. Labrador, H. Hing and G. J. Bashaw (2003). "Slit stimulation recruits Dock and Pak to the roundabout receptor and increases Rac activity to regulate axon repulsion at the CNS midline." Neuron 40(1): 113-27.

Fricke, C., J. S. Lee, S. Geiger-Rudolph, F. Bonhoeffer and C. B. Chien (2001). "astray, a zebrafish roundabout homolog required for retinal axon guidance." Science 292(5516): 507-10.

Fukuhara, N., J. A. Howitt, S. A. Hussain and E. Hohenester (2008). "Structural and functional analysis of slit and heparin binding to immunoglobulin-like domains 1 and 2 of Drosophila Robo." J Biol Chem 283(23): 16226-34.

Haffter, P., M. Granato, M. Brand, M. C. Mullins, M. Hammerschmidt, D. A. Kane, J. Odenthal, F. J. van Eeden, Y. J. Jiang, C. P. Heisenberg, R. N. Kelsh, M. Furutani-Seiki, E. Vogelsang, D. Beuchle, U. Schach, C. Fabian and C. Nusslein-Volhard (1996). "The identification of genes with unique and essential functions in the development of the zebrafish, Danio rerio." Development 123: 1-36.

Howitt, J. A., N. J. Clout and E. Hohenester (2004). "Binding site for Robo receptors revealed by dissection of the leucine-rich repeat region of Slit." Embo J 23(22): 4406-12.

Hu, H. (2001). "Cell-surface heparan sulfate is involved in the repulsive guidance activities of Slit2 protein." Nat Neurosci 4(7): 695-701.

Hu, H., M. Li, J. P. Labrador, J. McEwen, E. C. Lai, C. S. Goodman and G. J. Bashaw (2005). "Cross GTPase-activating protein (CrossGAP)/Vilse links the Roundabout receptor to Rac to regulate midline repulsion." Proc Natl Acad Sci U S A 102(12): 4613-8.

Hussain, S. A., M. Piper, N. Fukuhara, L. Strochlic, G. Cho, J. A. Howitt, Y. Ahmed, A. K. Powell, J. E. Turnbull, C. E. Holt and E. Hohenester (2006). "A molecular mechanism for the heparan sulfate dependence of slit-robo signaling." J Biol Chem 281(51): 39693-8.

Hutson, L. D. and C. B. Chien (2002a). "Pathfinding and error correction by retinal axons: the role of astray/robo2." Neuron 33(2): 205-17.

Hutson, L. D. and C. B. Chien (2002b). "Wiring the zebrafish: axon guidance and synaptogenesis." Curr Opin Neurobiol 12(1): 87-92.

Hutson, L. D., M. J. Jurynec, S. Y. Yeo, H. Okamoto and C. B. Chien (2003). "Two divergent slit1 genes in zebrafish." Dev Dyn 228(3): 358-69.

Inatani, M., F. Irie, A. S. Plump, M. Tessier-Lavigne and Y. Yamaguchi (2003). "Mammalian brain morphogenesis and midline axon guidance require heparan sulfate." Science 302(5647): 1044-6.

Itoh, A., T. Miyabayashi, M. Ohno and S. Sakano (1998). "Cloning and expressions of three mammalian homologues of Drosophila slit suggest possible roles for Slit in the formation and maintenance of the nervous system." Brain Res Mol Brain Res 62(2): 175-86.

Karlstrom, R. O., T. Trowe, S. Klostermann, H. Baier, M. Brand, A. D. Crawford, B. Grunewald, P. Haffter, H. Hoffmann, S. U. Meyer, B. K. Muller, S. Richter, F. J. van Eeden, C. Nusslein-Volhard and F. Bonhoeffer (1996). "Zebrafish mutations affecting retinotectal axon pathfinding." Development 123: 427-38.

Keleman, K., S. Rajagopalan, D. Cleppien, D. Teis, K. Paiha, L. A. Huber, G. M. Technau and B. J. Dickson (2002). "Comm sorts robo to control axon guidance at the Drosophila midline." Cell 110(4): 415-27.

Kidd, T., C. Russell, C. S. Goodman and G. Tear (1998a). "Dosage-sensitive and complementary functions of roundabout and commissureless control axon crossing of the CNS midline." Neuron 20(1): 25-33.

Kidd, T., K. Brose, K. J. Mitchell, R. D. Fetter, M. Tessier-Lavigne, C. S. Goodman and G. Tear (1998b). "Roundabout controls axon crossing of the CNS midline and defines a novel subfamily of evolutionarily conserved guidance receptors." Cell 92(2): 205-15.

Kidd, T., K. S. Bland and C. S. Goodman (1999). "Slit is the midline repellent for the robo receptor in Drosophila." Cell 96(6): 785-94.

Lee, J. S., R. Ray and C. B. Chien (2001). "Cloning and expression of three zebrafish roundabout homologs suggest roles in axon guidance and cell migration." Dev Dyn 221(2): 216-30.

Lee, J. S., S. von der Hardt, M. A. Rusch, S. E. Stringer, H. L. Stickney, W. S. Talbot, R. Geisler, C. Nusslein-Volhard, S. B. Selleck, C. B. Chien and H. Roehl (2004). "Axon sorting in the optic tract requires HSPG synthesis by ext2 (dackel) and extl3 (boxer)." Neuron 44(6): 947-60.

Li, X., Y. Chen, Y. Liu, J. Gao, F. Gao, M. Bartlam, J. Y. Wu and Z. Rao (2006). "Structural basis of Robo proline-rich motif recognition by the srGAP1 Src homology 3 domain in the Slit-Robo signaling pathway." J Biol Chem 281(38): 28430-7.

Liu, Z., K. Patel, H. Schmidt, W. Andrews, A. Pini and V. Sundaresan (2004). "Extracellular Ig domains 1 and 2 of Robo are important for ligand (Slit) binding." Mol Cell Neurosci 26(2): 232-40.

Lundstrom, A., M. Gallio, C. Englund, P. Steneberg, J. Hemphala, P. Aspenstrom, K. Keleman, L. Falileeva, B. J. Dickson and C. Samakovlis (2004). "Vilse, a conserved Rac/Cdc42 GAP mediating Robo repulsion in tracheal cells and axons." Genes Dev 18(17): 2161-71.

Nguyen Ba-Charvet, K. T., K. Brose, L. Ma, K. H. Wang, V. Marillat, C. Sotelo, M. Tessier-Lavigne and A. Chedotal (2001). "Diversity and specificity of actions of Slit2 proteolytic fragments in axon guidance." J Neurosci 21(12): 4281-9.

Niclou, S. P., L. Jia and J. A. Raper (2000). "Slit2 is a repellent for retinal ganglion cell axons." J Neurosci 20(13): 4962-74.

Plump, A. S., L. Erskine, C. Sabatier, K. Brose, C. J. Epstein, C. S. Goodman, C. A. Mason and M. Tessier-Lavigne (2002). "Slit1 and Slit2 cooperate to prevent premature midline crossing of retinal axons in the mouse visual system." Neuron 33(2): 219-32.

Rajagopalan, S., E. Nicolas, V. Vivancos, J. Berger and B. J. Dickson (2000a). "Crossing the midline: roles and regulation of Robo receptors." Neuron 28(3): 767-77.

Rajagopalan, S., V. Vivancos, E. Nicolas and B. J. Dickson (2000b). "Selecting a longitudinal pathway: Robo receptors specify the lateral position of axons in the Drosophila CNS." Cell 103(7): 1033-45.

Rasband, K., M. Hardy and C. B. Chien (2003). "Generating X: formation of the optic chiasm." Neuron 39(6): 885-8.

Rhee, J., N. S. Mahfooz, C. Arregui, J. Lilien, J. Balsamo and M. F. VanBerkum (2002). "Activation of the repulsive receptor Roundabout inhibits N-cadherin-mediated cell adhesion." Nat Cell Biol 4(10): 798-805.

Rhiner, C., S. Gysi, E. Frohli, M. O. Hengartner and A. Hajnal (2005). "Syndecan regulates cell migration and axon guidance in C. elegans." Development 132(20): 4621-33.

Ringstedt, T., J. E. Braisted, K. Brose, T. Kidd, C. Goodman, M. Tessier-Lavigne and D. D. O'Leary (2000). "Slit inhibition of retinal axon growth and its role in retinal axon pathfinding and innervation patterns in the diencephalon." J Neurosci 20(13): 4983-91.

Ronca, F., J. S. Andersen, V. Paech and R. U. Margolis (2001). "Characterization of Slit protein interactions with glypican-1." J Biol Chem 276(31): 29141-7.

Rothberg, J. M., D. A. Hartley, Z. Walther and S. Artavanis-Tsakonas (1988). "slit: an EGF-homologous locus of D. melanogaster involved in the development of the embryonic central nervous system." Cell 55(6): 1047-59.

Rothberg, J. M., J. R. Jacobs, C. S. Goodman and S. Artavanis-Tsakonas (1990). "slit: an extracellular protein necessary for development of midline glia and commissural axon pathways contains both EGF and LRR domains." Genes Dev 4(12A): 2169-87.

Seeger, M., G. Tear, D. Ferres-Marco and C. S. Goodman (1993). "Mutations affecting growth cone guidance in Drosophila: genes necessary for guidance toward or away from the midline." Neuron 10(3): 409-26.

Simpson, J. H., K. S. Bland, R. D. Fetter and C. S. Goodman (2000a). "Short-range and long-range guidance by Slit and its Robo receptors: a combinatorial code of Robo receptors controls lateral position." Cell 103(7): 1019-32.

Simpson, J. H., T. Kidd, K. S. Bland and C. S. Goodman (2000b). "Short-range and long-range guidance by slit and its Robo receptors. Robo and Robo2 play distinct roles in midline guidance." Neuron 28(3): 753-66.

Steigemann, P., A. Molitor, S. Fellert, H. Jackle and G. Vorbruggen (2004). "Heparan sulfate proteoglycan syndecan promotes axonal and myotube guidance by slit/robo signaling." Curr Biol 14(3): 225-30.

Stuermer, C. A. (1988). "Retinotopic organization of the developing retinotectal projection in the zebrafish embryo." J Neurosci 8(12): 4513-30.

Tear, G., R. Harris, S. Sutaria, K. Kilomanski, C. S. Goodman and M. A. Seeger (1996). "commissureless controls growth cone guidance across the CNS midline in Drosophila and encodes a novel membrane protein." Neuron 16(3): 501-14.

Trowe, T., S. Klostermann, H. Baier, M. Granato, A. D. Crawford, B. Grunewald, H. Hoffmann, R. O. Karlstrom, S. U. Meyer, B. Muller, S. Richter, C. Nusslein-Volhard and F. Bonhoeffer (1996). "Mutations disrupting the ordering and

topographic mapping of axons in the retinotectal projection of the zebrafish, Danio rerio." Development 123: 439-50.

Wang, K. H., K. Brose, D. Arnott, T. Kidd, C. S. Goodman, W. Henzel and M. Tessier-Lavigne (1999). "Biochemical purification of a mammalian slit protein as a positive regulator of sensory axon elongation and branching." Cell 96(6): 771-84.

Whitford, K. L., V. Marillat, E. Stein, C. S. Goodman, M. Tessier-Lavigne, A. Chedotal and A. Ghosh (2002). "Regulation of cortical dendrite development by Slit-Robo interactions." Neuron 33(1): 47-61.

Wilson, S. W., L. S. Ross, T. Parrett and S. S. Easter, Jr. (1990). "The development of a simple scaffold of axon tracts in the brain of the embryonic zebrafish, Brachydanio rerio." Development 108(1): 121-45.

Wong, K., X. R. Ren, Y. Z. Huang, Y. Xie, G. Liu, H. Saito, H. Tang, L. Wen, S. M. Brady-Kalnay, L. Mei, J. Y. Wu, W. C. Xiong and Y. Rao (2001). "Signal transduction in neuronal migration: roles of GTPase activating proteins and the small GTPase Cdc42 in the Slit-Robo pathway." Cell 107(2): 209-21.

Yang, L. and G. J. Bashaw (2006). "Son of sevenless directly links the Robo receptor to rac activation to control axon repulsion at the midline." Neuron 52(4): 595-

CHAPTER 2

SLIT2 INDUCES COLLAPSE OF RGC GROWTH CONES THROUGH THE ASTRAY (ROBO2) RECEPTOR IN VITRO

Abstract

The identification of axon guidance cues and their receptors has been a great step forward in furthering our understanding of early nervous system development. The large secreted Slits make up one family of these signaling molecules. They and their receptors, the Robos, have been shown to be important in axon guidance in several systems. These molecules were initially identified and best understood in *Drosophila*, but much has also been learned in vertebrates, particularly in the guidance of retinal axons, where the repellent Slits are thought to act as guardrails to keep developing axons on the proper pathway. There is still much to learn about Slit-Robo signaling. Although Slits have been shown to act through Robos in *Drosophila*, this has not been formally proven in vertebrates. Our knowledge of the molecules that are important for transducing the signal to cause cytoskeletal changes is incomplete. Finally, in zebrafish the expression pattern of Slit1a is not consistent with its acting as a simple repellent for axon guidance. In this chapter, I have developed a retinal explant culture system to confirm that Slit2 acts to collapse zebrafish retinal ganglion cell growth cones. Also, by performing these collapse assays on explants derived from *robo2* mutants, I have shown that this Slit2-mediated collapse requires the Robo2 receptor.

Introduction

Slit was first identified in *Drosophila* (Rothberg et al., 1988) and later shown to be a repulsive axon guidance cue (Kidd et al., 1999). It was subsequently cloned and shown to encode a 1480 residue protein that is secreted by midline glia (Rothberg et al., 1990). Mammals have 3 *slit* genes (*slit1-3*). In both vertebrates and invertebrates, Robos

are thought to act as receptors for Slits, and all Robos tested to date have been shown to bind to all Slits biochemically (Brose et al., 1999; Simpson et al., 2000). *Drosophila* Slit is unusual in that it contains 4 Leucine Rich Repeats (LRRs) and 7 Epidermal Growth Factor (EGF) motifs; only one or the other of these protein-protein interaction domains is typically found in a given protein. In *Drosophila*, Slit is expressed in a broad band at the midline and has been shown to function as a 'gatekeeper', determining which axons may cross (Kidd et al., 1998). At the midline of the vertebrate visual system, multiple Slits are expressed in bands that lie perpendicular to the midline. This is consistent with these Slits acting as repellent guardrails to keep axons from straying. At the mouse optic chiasm, single mutations in *slit1* or *slit2* yield little if any phenotype, but the *slit1; slit2* double mutant forms two commissures instead of the normal optic chiasm (Plump et al., 2002). This is consistent with repulsion by Slits, given the overlapping regions of Slit1 and Slit2 expression that border the optic chiasm (Rasband et al., 2003).

Slits are generally thought to have a repellent effect in both cell migration and axon guidance (Brose et al., 2000). However, Slit is also reported to induce axon branching of certain neurons (Whitford et al., 2002; Wang et al., 1999). Axon branching is not strictly the same as attraction, but it is considered to be a positive effect and is certainly very different from repulsion. The 190 kD Slit2 is the best characterized of the vertebrate Slits, and has been shown to be proteolytically cleaved into a 140kD N-terminal fragment and a smaller 60kD C-terminal piece (Figure 1.1). Both uncleaved Slit2 and the N-terminal fragment have biological function, binding to Robos and acting as repellents (Brose et al., 1999). The smaller C-terminal fragment differs in being freely diffusible, and has no known function. In culture, Slit2 has been shown to collapse retinal

ganglion cell (RGC) growth cones in chick (Niclou et al., 2000), rat (Ringstedt et al., 2000), and mouse (Erskine et al., 2000). Similarly, Slit1 causes collapse of mouse RGC growth cones (Plump et al., 2002).

In the zebrafish optic chiasm, the expression of Slit2 and Slit3 is similar to the mouse expression of Slit1 and Slit2 (Figure 1.2). In zebrafish, about one-third of genes have been duplicated as a result of a genomewide duplication. Duplication of *slit1* resulted in *slit1a* and *slit1b* (Hutson et al., 2003), yielding together with *slit2* and *slit3* a total of 4 zebrafish *slit* genes. While *slit1b* is not expressed in the visual pathway, *slit1a* has a very interesting expression pattern, being expressed in a broad domain underneath the optic tract (Hardy and Chien, unpublished data). This expression is not easily reconciled with *slit1a* functioning as a simple repellent. Morpholino knockdown and overexpression data also imply that *slit1a* may have a novel (nonrepellent) function in the optic tract of the zebrafish (Hardy and Chien, unpublished data).

Another signaling pathway, SDF-1-CXCR4, has been shown to modulate the proper level of Slit-Robo signaling in vivo (Chalasani et al., 2003a,b). Interestingly, knockdown of SDF-1 only affects Robo signaling in the hypomorphic *te284* allele but not in the null allele *ti272z* (Chalasani et al., 2007). This is presumably because loss of SDF-1 upregulates Robo2 function in *te284*, while the null allele completely lacks functional receptor, so that the level of Robo signaling cannot be upregulated.

In this chapter, I perform in vitro assays to see if Slits are acting to collapse zebrafish RGC growth cones. I then test whether Slit2 induced collapse requires the Astray (Robo2) receptor. I also tried to determine the effect of Slit1a on RGCs but these experiments were unsuccessful due to the inability to obtain sufficient Slit1a protein.

Finally, as part of a collaboration with Jonathan Raper's laboratory, I performed an analysis to test the effects of SDF-1 on Slit induced collapse in zebrafish RGCs.

Materials and Methods

Eye Dissection and Retinal Explants

Embryos were collected after fertilization and bleached in 0.038% bleach for five minutes. Whole eyes were dissected at ~30 hpf with electrolytically-sharpened tungsten needles in culture media. The eyes were rinsed several times, then cut into several pieces and explanted overnight at 28.5°C on glass. The glass coverslips were treated with 10μg/mL Poly-D-Lysine (Sigma P0899) for three hours, and then treated with Laminin (Sigma L2020) for 3 hours before culturing (10 μg/mL in culture media). Cutting the eyes promotes better attachment of the explant to the substrate and facilitates axons exiting the eye. They were cultured in media comprised of 70% Leibovitz's L-15 (Sigma L4386-10X1L), plus 1x N2-Supplement (Invitrogen 17502-048) and gentamycin (10 μg/mL). N2-Supplement is chemically defined and there is no serum present in this culture media. If used within a week, adding glutamine does not seem to be necessary.

Fixed Analysis of Collapse

For the fixed analysis, retinal explants were placed on treated glass coverslips and cultured in the bottom of a well containing 500μL of media. Conditioned media was collected from two stably transfected cell lines. These cell lines express human Slit2-GFP or GFP alone as a control. A large batch of conditioned media was collected and

aliquoted so that the conditioned media would always undergo exactly one freeze/thaw cycle.

To each culture was carefully added 200μL total volume containing from 0 to 200μL of Slit-GFP conditioned media and the rest of the volume (200-0 μL) made up from GFP conditioned media. After 15 minutes the cultures were fixed by adding 500μL of 4% PFA. To assay the timecourse of collapse, 200μL of Slit-GFP conditioned media was added and then fixed with 4% PFA after ~0, 5, 10, 20, or 30 minutes.

Live Imaging of Collapse

For live imaging, explants were cultured on glass bottom 35mm dishes that had been treated (as before) with Polylysine and Laminin in 4mL of media. Cultures were imaged using phase microscopy with a prewarmed stage. Images were captured every 1 or 2 minutes for 15 minutes to get a baseline of each growth cone's behavior. Growth cones that behaved erratically or were completely static during this time were not included in the analysis. After 15 minutes, the partially purified Slit (or control) was carefully added to the culures and mixed gently by pipetting. From 10-100μL of partially purified Slit (or control) was added to each culture and imaging was continued for up to one hour.

Slit Constructs and Transfections

For the hSlit2 analysis, conditioned media was obtained from stably transfected cell lines provided from Yi Rao (Northwestern University). The zebrafish Slit constructs were transfected into HEK293T cells.

Slit Purification for Live Analysis

To partially purify Slit, the transfected cells are rinsed with PBS and then incubated twice with a high salt buffer (1M NaCl 10mM HEPES 1x protease inhibitors) to strip proteins from the cell membrane. These extracts were combined and centrifuged to remove debris then passed through a concentrator column (Amicon Ultra UFC910024) that reduced the volume from 12mL down to 100-200μL. The resulting extract was then dialyzed in 70% L15 media to reduce the salt concentration.

Bradford Assays and Western Blots

For every round of transfection and protein purification, three constructs (GFP only, Slit1a-GFP, and Slit2-GFP) were always processed side by side at the same conditions. After dialysis, a Bradford analysis was performed to determine total protein levels. Then an aliquot of the extract was tested by Western blot using an anti-GFP antibody.

SDF and CXCR4

To test SDF-1 effects on hSlit2-mediated collapse, culture and collapse assays were performed as in the fixed analysis above. For each condition, a solution of conditioned media (composed of hSlit2 and/or control) and SDF-1 was prepared then added to the explant cultures. Human SDF-1 had an effect in chick cultures at 100 ng/mL (Chalasani et al., 2003a,b) but only had a weak effect on zebrafish RGCs at this concentration, so I also tried increasing the concentration 10 fold.

Results

Human Slit2 Collapses Zebrafish RGC Growth Cones

In many systems, Slits have been demonstrated to be a repellent signal for developing axons. Specifically, Slit2 has been shown to be repulsive in culture for RGCs derived from chick (Niclou et al., 2000), rat (Ringstedt et al., 2000), and mouse (Erskine et al., 2000). Slit1 has also been demonstrated to collapse RGC axons in mouse (Plump et al., 2002). At the zebrafish optic chiasm, the combined expression pattern of Slit2 and Slit3 in vivo is very similar to the combined expression of Slit1 and Slit2 in mouse (Figure 1.2) and both of these are consistent with Slits acting as repellent 'guardrails' to keep developing axons on the proper pathway. To test whether zebrafish Slit2 acts in a repellent manner similar to what is seen in other vertebrates, we performed a series of collapse assays.

In these experiments, growth cones from RGC explants were challenged with either conditioned medium containing human Slit2, or medium from untransfected HEK cells, or a combination of these media. The explants were then fixed with PFA and scored for collapse using phase microscopy. It should be mentioned that the zebrafish RGC explant conditions have not been optimized over decades, and so the resulting lack of robust axonal outgrowth requires the pooling of large numbers of explants. In scoring collapse, growth cones were only counted if they had grown at least 50μm from the body of the explant and if they were well-separated from other axons. For an example of an explant and collapsed and uncollapsed growth cones (Figure 2.1 A, B). To determine the optimum time-point for measuring collapse, I fixed the explants at various times after

adding the conditioned media, and obtained a timecourse of collapse (Figure 2.1 C). The background level of collapse was 30-40% of axons with collapsed growth cones. This was consistently seen in both explants exposed to only control media or those exposed to no conditioned media at all. As soon as 5 minutes after adding Slit-containing conditioned media, the explants showed an increase in collapse to 55%. The maximum level of collapse was 70-80% and was seen as early as 10 minutes after adding conditioned media.

It is difficult to quantify the concentration of Slit protein in the conditioned media, and the amount could easily vary from batch to batch. To reduce variability, the data shown are obtained from a single large batch of conditioned media. Aliquots were frozen at –80°C so that any given experiment was done with Slit that has undergone exactly one freeze/thaw cycle; Slit function is reported to be highly vulnerable to repetitive freeze/thaw cycles (J. Raper, personal communication). To each culture, originally containing 500μL of culture media, conditioned media was added which contained from 0-200μL of Slit2 conditioned medium combined with enough control media to make a total volume of 200μL. When pure control medium was added to the cultures, the result was 35% collapse, as expected from the background level of collapse of these RGC explants. When pure conditioned medium was added, 70% of growth cones were collapsed. Adding increasing fractions of Slit media resulted in increasing levels of collapse (Figure 2.1 D). Thus, human Slit2 acts to induce collapse in zebrafish RGCs in a dose-dependent manner.

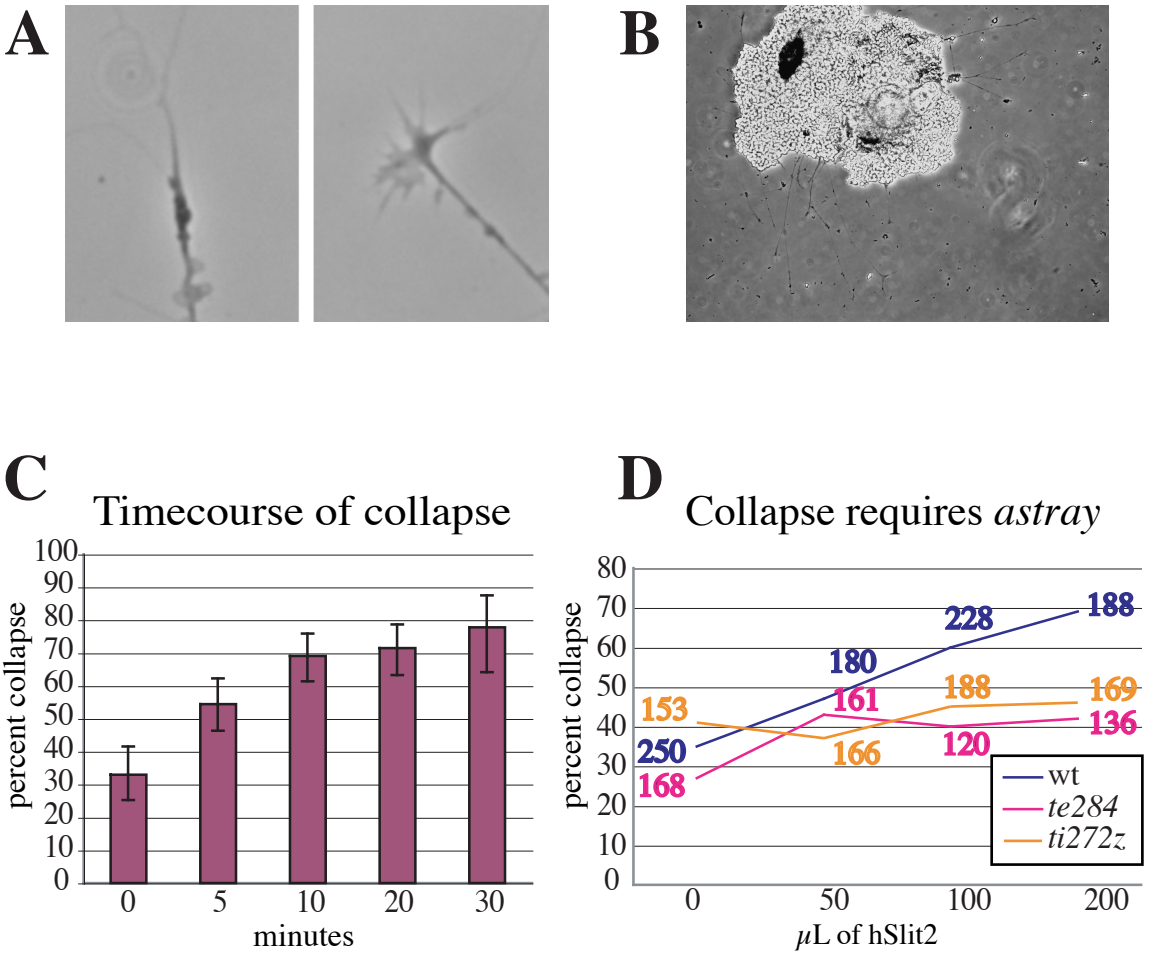

Figure 2.1 hSlit2 Collapse Assay. (A) Example of collapsed (left) and uncollapsed (right) growth cones. (B) A cultured retinal explant. (C) Graph showing the timecourse of collapse. (D) The collapse of three genotypes in response to hSlit2. The numbers are growth cones scored at each condition. hSlit2 causes collapse of wildtype growth cones in a dose dependent manner. This hSlit2 collapse requires the astray receptor, as explants from either *te284* or *ti272z* embryos show no increase in collapse in response to hSlit2.

The Astray Receptor Is Required for hSlit2 Collapse

Having demonstrated that Slit2 induces collapse, I next tested whether this collapse was mediated by the Astray receptor (Robo2), by performing collapse assay experiments on retinal explants derived from *astray* embryos. Two alleles of astray were tested. The *ti272z* mutation encodes a premature stop codon before the transmembrane domain, rendering it completely unable to function as a receptor (Fricke et al., 2001). These animals lack any functioning receptor and so their growth cones should not be able to detect the presence of Slit (Figure 2.1 D). The *te284* allele encodes a missense mutation within the transmembrane domain. The retinal axon guidance phenotype of *te284* homozygotes is fully penetrant, but weaker on average than *ti272z* homozygotes, so I was curious whether I could detect any increase in the collapse of *te284* growth cones compared to *ti272z*.

These experiments showed that the Astray receptor is indeed required for Slit2 mediated collapse and that both alleles respond similarly (Figure 2.1 D). Even when presented with a concentration of Slit conditioned media that induces a collapse of 70% of wildtype axons, both *ti272z* and *te284* axons showed collapse of just over 40%. This demonstrates directly that Slit2 signaling requires the Astray receptor.

Zebrafish Slit2 Causes RGC Growth Cone Collapse

These initial collapse assay experiments were done using human Slit2. From the high sequence conservation between human and zebrafish Slit proteins (Figure 1.2 D), I expected that zebrafish Slit2 would also collapse zebrafish RGC growth cones, and likely

be more potent than human Slit2. To improve the statistical power of the collapse assay, I replaced the fixed analysis with the more painstaking approach of imaging live growth cones before and after addition of conditioned media. I hoped to not only use fewer explants, but to be able to discern subtle changes in growth cone behavior. I also adopted a new protocol to obtain partially purified Slit protein from transfected cells, rather than conditioned media as before. This protocol used high salt buffer to strip proteins off cell membranes. These high salt extracts were then concentrated and partially purified by centrifugation in concentrator columns. Another difference was that I was now obtaining Slit from transient transfections instead of the stably transfected cell lines used in the human Slit collapse experiments.

Adding zebrafish Slit2 to the cultures resulted in increased collapse even at a low concentration (Figure 2.2). For controls, I used both a mock transfected extract and high salt buffer (to control for effects due to salt concentration). Neither control extract caused any increase in collapse until it was added at a very high concentration. This shows that zebrafish Slit2 also causes collapse of RGC axons.

Detecting Slit Proteins and Troubleshooting

In addition to zebrafish Slit2, I also wanted to test the function of zebrafish Slit1a, especially since its expression pattern suggests that it does not act as a simple repellent in the zebrafish visual pathway. Unfortunately, I was unable to consistently obtain Slit1a protein.

I optimized the transfection step using several different cell lines. I eventually chose a HEK293T cell line that bears a copy of the SV40 large T antigen and appeared to

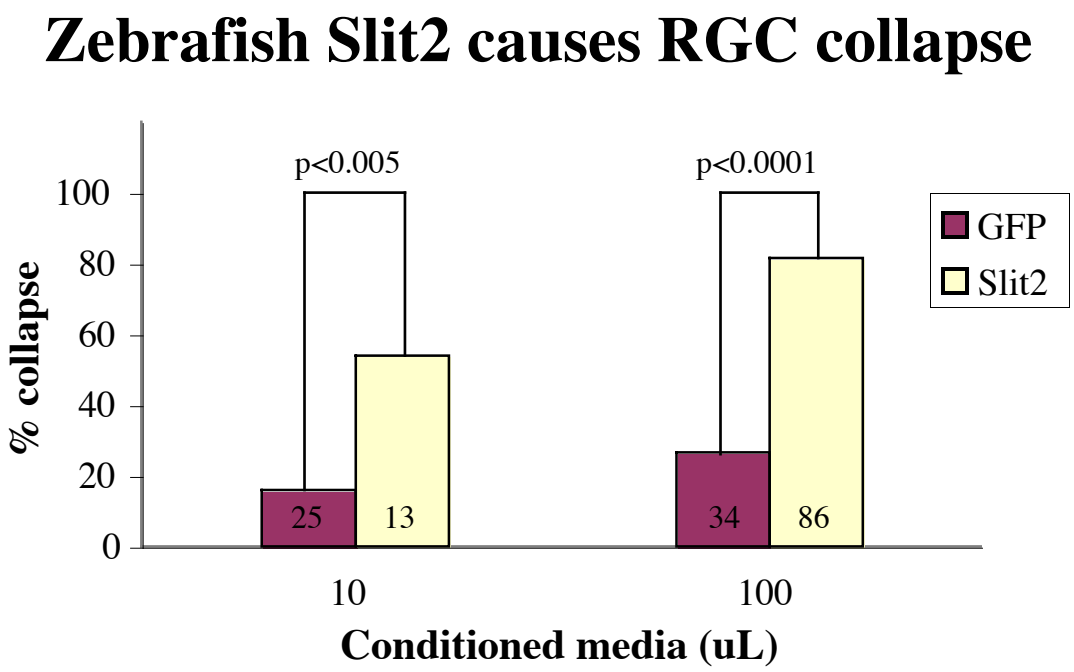

Figure 2.2 Zebrafish Slit2 Causes Collapse of RGC Growth Cones. Partially purified cmv:Slit2-GFP protein (yellow) causes increased collapse compared to partially purified cmv:GFP protein (purple). Amount added is the volume (in μL) added to an explant with 2mL of culture media. The n for each condition represents pooling from several experiments.

produce high levels of Slit1a-GFP protein based on GFP expression. I also tried using several different Slit1a constructs using different promoters. Frustratingly, the Slit1a constructs gave highly variable yields of protein even though the corresponding Slit2 constructs worked well. I also tried troubleshooting at every step of the purification protocol, including different centrifugation regimens at the concentration step, and adding a dialysis step to remove the high salt used for stripping Slit protein from cell membranes.

For each batch of protein, I collected three samples produced with the same transfection conditions: GFP only as a control, the Slit1a-GFP construct, and the Slit2-GFP construct. After each purification, I assayed total protein levels by performing a Bradford test, then running the extracts on a Western blot using anti-GFP antibody to assay specifically for Slits. I optimized the Slit2 purification significantly and was able to detect it easily by Western blot but was never able to reliably detect Slit1a by Western blot. Oddly, I was unable to detect Slit1a-GFP even in batches in which the transfected cells had fluoresced bright green, indicating that the DNA construct was correct and that protein was being made. To rule out that the cells were making Slit1a-GFP protein but were unable to export it properly, I tried lysing the cells using both physical means to disrupt the cells and chemical disruption with detergents, but was still unable to detect Slit1a-GFP by Western blots (Figure 2.3).

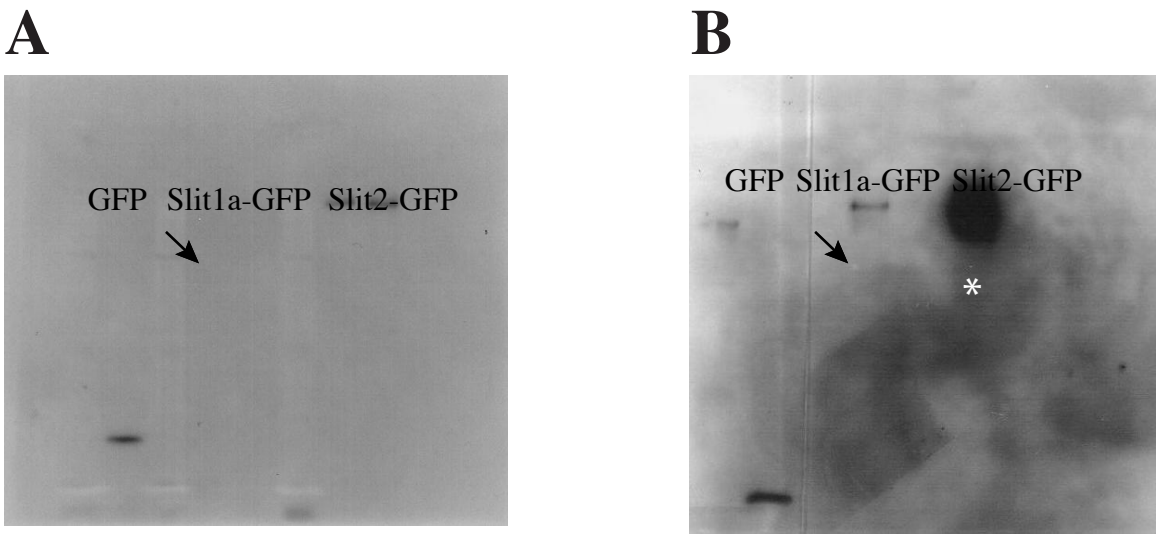

Figure 2.3 Western Blots Are Able to Detect GFP and Slit2-GFP But Not Slit1a-GFP reliably. (A) A Western blot that demonstrates GFP and Slit2-GFP protein are being made. Slit1-GFP protein is undetectable. Slit1a-GFP is approximately the same size as Slit2-GFP so if it were present we would see a similar band (arrows). (B) A Western blot that shows Slit1a-GFP (arrows) and Slit2-GFP (asterisk). This blot is done with a different round of Slit transfections. Slit1a-GFP and Slit2-GFP are both loaded at maximal amounts. This Western blot demonstrates that even in the uncommon transfections that give a band for Slit1a-GFP, the amounts of protein present is very low.

SDF-1 and CXCR4

SDF-1 and its receptor, CXCR4, have been shown to be important in modulating the level of Slit Robo signaling. CXCR4 is expressed in RGCs and SDF-1 can partially rescue the *astray* phenotype (Chalasani et al., 2003a,b). The rescue is only effective for the hypomorphic *te284* and not the null allele *ti272z* (Chalasani et al., 2007). This is most likely a result of SDF-1 being able to modulate Slit-Robo signaling in *te284* mutants, which have some level of Slit-Robo signaling, and not with the null *ti272z*, in which signaling is absent.

In collaboration with the Raper lab, whom were performing additional in vivo experiments, I first tested the effect of human SDF-1 on zebrafish RGCs in culture and determined that it does not induce collapse on its own (Figure 2.4). I then found that human SDF-1 did not significantly change hSlit2-induced collapse in wildtype explants at 100ng/ml, the concentration which had an effect in chick explants. Human SDF-1 is only 46% identical to zebrafish but is 71% identical to chick SDF-1. This may account for the fact that human SDF-1 at 100 ng/mL has an effect in modulating Slit collapse in RGCs of chick (Chalasani et al., 2003b) but not zebrafish (Figure 2.4). I reasoned that human SDF-1 might have some function in zebrafish RGCs with a severely reduced potency, so I repeated the experiment using higher levels of SDF-1. At a tenfold higher concentration, SDF-1 reduced the collapse caused by hSlit2 (Figure 2.4).

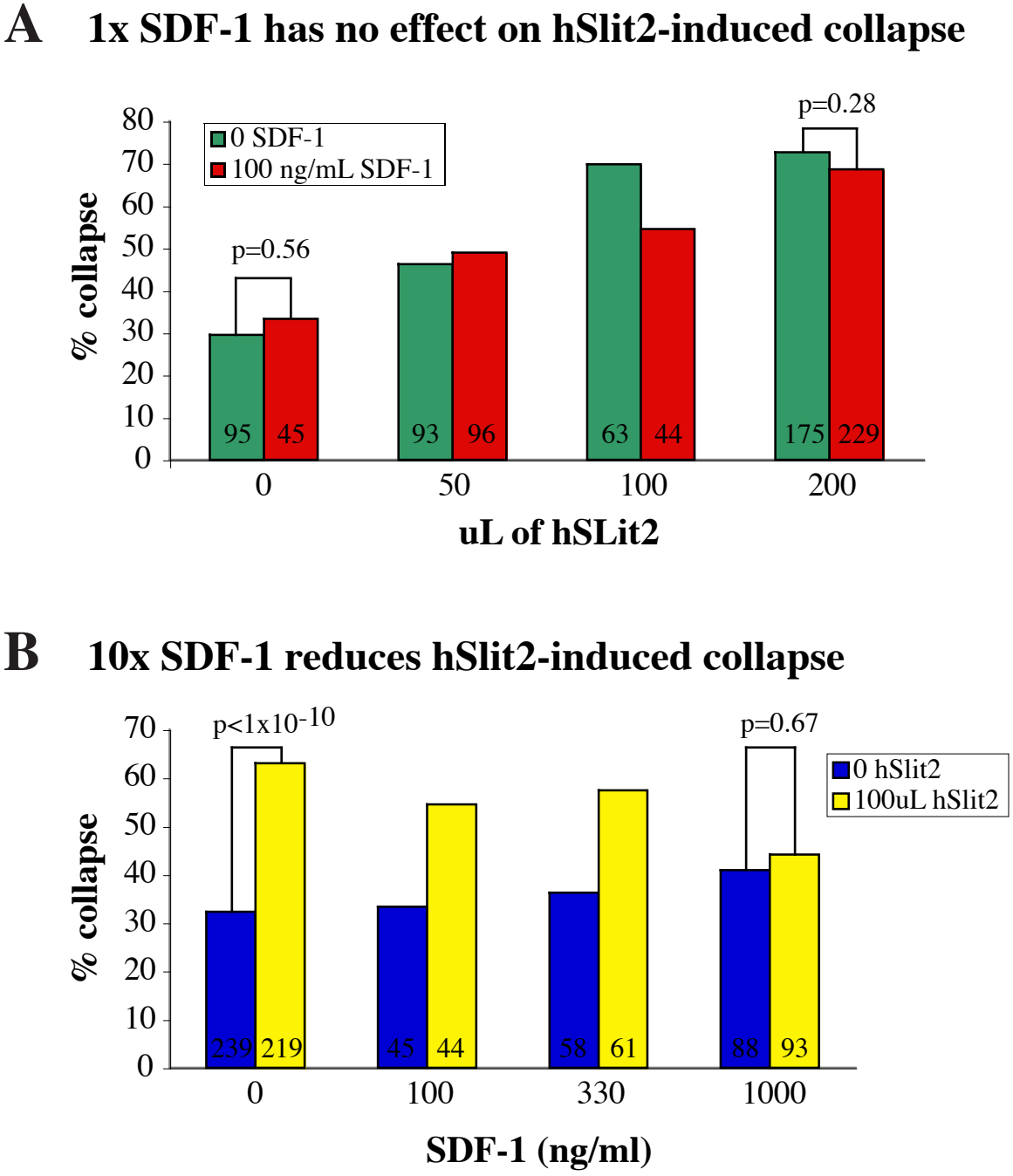

Figure 2.4 Human SDF-1 Only Reduces hSlit2 Induced Collapse of Zebrafish RGCs at High Concentrations. (A) Adding SDF-1 at 100 ng/mL does not significantly reduce the collapse induced by hSlit2 on zebrafish RGC growth cones. (B) At higher concentrations, SDF-1 is able to reduce hSlit2 induced collapse.

Discussion

Advantages of an In Vitro Approach

The strength of culture experiments lies in the ability to test directly the effect of a single variable. Conversely, the weakness of a culture approach is the use of artificial conditions, raising questions of biological relevance. My goal in these experiments was to develop in vitro assays for Slit function, to be combined later with in vivo experiments. There are several established assays for testing the function of guidance cues, which can largely be divided into collapse assays and turning assays. Turning assays are much more difficult to perform technically, and I did not finish establishing the necessary collagen gel explant co-cultures. The advantage would have been that turning assays can demonstrate either attraction or repulsion. The collapse assay does not test turning but collapse. Growth cone turning can be thought of as local collapse on one side of the growth cone in response to a gradient of a guidance cue. In collapse assays in which the guidance cue is present throughout the culture media, the growth cone does not detect differential levels of the guidance cue; instead, once high enough levels are present, the growth cone will collapse, since it cannot turn away from a higher concentration of the cue.

Slit2 Effects and Slit1a Difficulties

I showed for the first time that zebrafish RGC growth cones can be collapsed by Slit2 (either human or zebrafish). This was an expected result due to the evolutionary

conservation of Slits. More importantly, however, I was able to show that the Robo2 receptor is required for Slit2 induced collapse.

My other goal was to test what effects, if any, Slit1a might have on RGC growth cones. In zebrafish, the *slit1* gene has undergone a gene duplication leading to *slit1a* and *slit1b*. Such duplication events are potentially interesting because they can allow one duplicated gene to undergo functional evolution while the original function is maintained by the other duplicated gene. Slit1a may indeed be different from the other Slits. It is expressed in a broad domain underlying the optic tract, which is inconsistent with its acting as a simple repellent guidance cue (Hardy and Chien, unpublished data). Both morpholino knockdown and localized overexpression experiments also suggest that Slit1a may not be acting as a repellent in the optic tract (Hardy and Chien, unpublished data).

Considering these results, I was eager to test the effects of Slit1a in vitro, but was unable to obtain sufficient protein to perform the experiments. Initial transfections often yield limited Slit1a-GFP production based on GFP expression, and so I first tried optimizing the transfection reaction by varying concentrations of lipofectamine, CMV:Slit1a-GFP DNA, or both. I also tested transfections at different cell confluencies and letting the transfection proceed for different lengths of time. The most significant increase in transfection efficiency came from switching to a HEK293T cell line. Optimizing these parameters resulted in reliable protein production (based on GFP expression in Westerns) from both the GFP control and Slit2-GFP constructs, but not from the Slit1a-GFP construct. I then tried several constructs using different promoters, but all of these were similar in giving good levels of Slit2 but variable levels of Slit1a.

Another problem seemed to be in the Slit purification protocol. This protocol uses a high salt wash to strip protein off the cell surfaces, then concentrating by spinning through a concentrator column. I added an additional dialysis step to replace the high salt solution with culture medium because growth cones are likely sensitive to the high salt. After a Bradford assay to determine total protein concentration, I performed Western blots to specifically measure the presence of Slit-GFP protein. Even when Slit1a-GFP transfected cells glowed brightly, I was unable to detect a band for Slit1a-GFP on the Western. Slit2-GFP and the GFP transfections, showed up brightly on Westerns. Sometimes I detected a faint band after loading large volumes of Slit1a-GFP extract, but not consistently. We even tried to lyse the transfected cells by several different methods to see if the inability to detect Slit1a-GFP by Western blot was due to a failure in exporting the protein; we were still unable to detect Slit1a-GFP in the lysate. Although Slit proteins are large and considered hard to work with, it is unclear why Slit1a would be so problematic when we were able to get satisfactory results for Slit2.

Future Directions

In future, there are several in vitro experiments that would be interesting to follow up on. One would be to repeat these collapse experiments with other alleles of *astray* to search for ones with an impaired Slit response. Some of the weak alleles from the screen presented in Chapter 3 would make interesting candidates.

There still remain questions about Slit1a function based on its expression and other experimental results and it could still be informative to perform these experiments

if some reliable means of obtaining good quality protein were found. It would also be a useful way to test if Slit1a also acts through the Astray receptor.

As with SDF-1 and CXCR4, the collapse assays can be expanded to test the requirements of other molecules on the Slit Robo signaling pathway. For example, one could use morpholinos to test what effects removing function of candidate downstream signaling genes has on Slit induced collapse.

References

Brose, K., K. S. Bland, K. H. Wang, D. Arnott, W. Henzel, C. S. Goodman, M. Tessier-Lavigne and T. Kidd (1999). "Slit proteins bind Robo receptors and have an evolutionarily conserved role in repulsive axon guidance." Cell 96(6): 795-806.

Brose, K. and M. Tessier-Lavigne (2000). "Slit proteins: key regulators of axon guidance, axonal branching, and cell migration." Curr Opin Neurobiol 10(1): 95-102.

Chalasani, S. H., F. Baribaud, C. M. Coughlan, M. J. Sunshine, V. M. Lee, R. W. Doms, D. R. Littman and J. A. Raper (2003a). "The chemokine stromal cell-derived factor-1 promotes the survival of embryonic retinal ganglion cells." J Neurosci 23(11): 4601-12.

Chalasani, S. H., K. A. Sabelko, M. J. Sunshine, D. R. Littman and J. A. Raper (2003b). "A chemokine, SDF-1, reduces the effectiveness of multiple axonal repellents and is required for normal axon pathfinding." J Neurosci 23(4): 1360-71.

Chalasani, S. H., A. Sabol, H. Xu, M. A. Gyda, K. Rasband, M. Granato, C. B. Chien and J. A. Raper (2007). "Stromal cell-derived factor-1 antagonizes slit/robo signaling in vivo." J Neurosci 27(5): 973-80.

Erskine, L., S. E. Williams, K. Brose, T. Kidd, R. A. Rachel, C. S. Goodman, M. Tessier-Lavigne and C. A. Mason (2000). "Retinal ganglion cell axon guidance in the mouse optic chiasm: expression and function of robos and slits." J Neurosci 20(13): 4975-82.

Fricke, C., J. S. Lee, S. Geiger-Rudolph, F. Bonhoeffer and C. B. Chien (2001). "astray, a zebrafish roundabout homolog required for retinal axon guidance." Science 292(5516): 507-10.

Hutson, L. D., M. J. Jurynec, S. Y. Yeo, H. Okamoto and C. B. Chien (2003). "Two divergent slit1 genes in zebrafish." Dev Dyn 228(3): 358-69.

Kidd, T., K. S. Bland and C. S. Goodman (1999). "Slit is the midline repellent for the robo receptor in Drosophila." Cell 96(6): 785-94.

Kidd, T., K. Brose, K. J. Mitchell, R. D. Fetter, M. Tessier-Lavigne, C. S. Goodman and G. Tear (1998). "Roundabout controls axon crossing of the CNS midline and defines a novel subfamily of evolutionarily conserved guidance receptors." Cell 92(2): 205-15.

Niclou, S. P., L. Jia and J. A. Raper (2000). "Slit2 is a repellent for retinal ganglion cell axons." J Neurosci 20(13): 4962-74.

Plump, A. S., L. Erskine, C. Sabatier, K. Brose, C. J. Epstein, C. S. Goodman, C. A. Mason and M. Tessier-Lavigne (2002). "Slit1 and Slit2 cooperate to prevent premature midline crossing of retinal axons in the mouse visual system." Neuron 33(2): 219-32.

Rasband, K., M. Hardy and C. B. Chien (2003). "Generating X: formation of the optic chiasm." Neuron 39(6): 885-8.

Ringstedt, T., J. E. Braisted, K. Brose, T. Kidd, C. Goodman, M. Tessier-Lavigne and D. D. O'Leary (2000). "Slit inhibition of retinal axon growth and its role in retinal axon pathfinding and innervation patterns in the diencephalon." J Neurosci 20(13): 4983-91.

Rothberg, J. M., D. A. Hartley, Z. Walther and S. Artavanis-Tsakonas (1988). "slit: an EGF-homologous locus of D. melanogaster involved in the development of the embryonic central nervous system." Cell 55(6): 1047-59.

Rothberg, J. M., J. R. Jacobs, C. S. Goodman and S. Artavanis-Tsakonas (1990). "slit: an extracellular protein necessary for development of midline glia and commissural axon pathways contains both EGF and LRR domains." Genes Dev 4(12A): 2169-87.

Simpson, J. H., T. Kidd, K. S. Bland and C. S. Goodman (2000). "Short-range and long-range guidance by slit and its Robo receptors. Robo and Robo2 play distinct roles in midline guidance." Neuron 28(3): 753-66.

Wang, K. H., K. Brose, D. Arnott, T. Kidd, C. S. Goodman, W. Henzel and M. Tessier-Lavigne (1999). "Biochemical purification of a mammalian slit protein as a positive regulator of sensory axon elongation and branching." Cell 96(6): 771-84.

Whitford, K. L., V. Marillat, E. Stein, C. S. Goodman, M. Tessier-Lavigne, A. Chedotal and A. Ghosh (2002). "Regulation of cortical dendrite development by Slit-Robo interactions." Neuron 33(1): 47-61.

CHAPTER 3

A NONCOMPLEMENTATION SCREEN TO ANALYZE ROBO2 SIGNALING

Abstract

The Robo2 receptor has been shown to be necessary for proper retinal pathfinding in the zebrafish. How the binding of Slit to this receptor is transduced to ultimately affect axon guidance is poorly understood, especially in vertebrates. Here we have performed a noncomplementation screen designed to further our understanding of *astray* signaling, seeking mutations in other genes that might show nonallelic noncomplementation, as well as new *astray* alleles. We were able to screen F1 offspring since *astray* is homozygous viable, fully penetrant, and recessive. We screened 21,649 haploid genomes and generated nine new *astray* alleles, which vary in the severity of their pathfinding errors. We have quantified their phenotypic strengths using an eight-point scoring method. Sequencing the *robo2* coding regions has identified the molecular lesion for five alleles. Two mutations lead to a protein that is truncated before the transmembrane domain, similar to the *ti272z* allele. The other three alleles encode missense mutations in the extracellular portion of the receptor. For the alleles with no identified mutation, in situ hybridization did not show any changes in Robo2 expression. Two of the weaker alleles, *zc13* and *zc19*, show a novel "empty tectum" phenotype, even in the absence of other pathfinding errors; this results from a retino-retinal projection. This forward genetic screen thus provides insights into Robo2 signaling in the vertebrate visual system.

Introduction

How the developing nervous system establishes its elaborate connections has long been an interesting problem. Over the past two decades, several families of axon

guidance molecules have been identified as being important in this development. One family of receptors is the Robo genes, which were first characterized in *Drosophila* (Seeger et al., 1993). Slits are the ligands for Robos and usually act as repulsive signals for projecting axons (Rothberg et al., 1988, 1990; Kidd et al., 1998a).

There are many systems that are currently used to study axon guidance, but the visual system of the zebrafish, *Danio rerio*, is a premier choice. Zebrafish are an established genetic system where large clutch sizes and relatively short generation time make them useful for performing genetic screens. In addition to a sequenced genome, many tools and protocols are available when working with zebrafish. External fertilization and transparent embryos are significant advantages for studying early developmental processes.

The visual system of zebrafish is well characterized (Stuermer, 1988; Wilson et al., 1990). Retinal axons are superficial and easily visualized. The first axons leave the eye through the optic nerve head at about 28 hours postfertilization (hpf) and reach the midline at 32 hpf, forming the optic chiasm with axons from the contralateral eye. After leaving the chiasm, the axons turn dorsally and caudally and travel through the optic tract before reaching their primary target, the optic tectum, at 48 hpf (Burrill and Easter, 1995).

The zebrafish mutant *astray*, which makes multiple pathfinding errors throughout this pathway, is defective in the zebrafish homolog of *robo2* (Fricke et al., 2001). Four alleles of *astray* were originally identified in a large-scale screen performed in Tübingen, Germany (Baier et al., 1996; Haffter et al., 1996; Karlstrom et al., 1996; Trowe et al., 1996). Of these, the null allele *ti272z* is the best characterized, and has been shown to be

required eye autonomously as expected for a guidance receptor molecule (Fricke et al., 2001).

It is poorly understood how the Astray receptor transduces its signal to guide the growing axon. Much of what is known about Robo signaling comes from work in *Drosophila*, where several genes such as *slit*, *ena*, and *abl* interact genetically with *robo*. The *comm* gene has also been shown to downregulate *robos* and is required for axons to cross the midline (Kidd et al., 1998a; Rajagopalan et al., 2000a). There are differences between Robo signaling in the fly and in the zebrafish visual system, which make studying this signaling pathway in a vertebrate important. In the vertebrate visual system, there are multiple *slit* genes but only a single *robo* gene expressed, whereas in *Drosophila* there are three *robo* genes and a single *slit* gene (Rajagopalan et al., 2000b; Lee et al., 2001). Also, in vertebrates there is no *comm* gene to downregulate *robo* expression, and the cytoplasmic domain of *robos* are poorly conserved between flies and vertebrates (Simpson et al., 2000).

To analyze Robo2 signaling, we took a forward-genetic approach, recovering genes that fail to complement *astray*. These mutations could be either new alleles of *astray* or alleles of genes that interact closely with *astray*, both of which should give insight into Robo2 signaling.

Materials and Methods

ENU Mutagenesis and Specific Locus Test

We generated mutagenized G0 males by fasting AB males, then placing them in phosphate buffered 3mM ENU (N-ethyl-N-nitrosourea) for 1 hour. This treatment was repeated weekly for 3 to 6 weeks. Then the fish were allowed to recover for 4 weeks before crossing them (Mullins et al., 1994; Solnica-Kreze et al., 1994). Each batch of G0s began with 30 healthy-looking males, but usually only about 10 fish survived the mutagenesis treatments.

We performed a specific locus test for each batch of G0s to determine the effectiveness of the ENU treatment. G0s were crossed to *gol/gol* females and the progeny were scored for the *golden* phenotype (Walker and Streisinger, 1983). Assuming that the mutagenesis conditions were similar for every G0 in a given batch, we combined numbers to get an approximate mutation rate, usually between 1 in 600 to 1 in 800. Outcrosses were performed to Tü or TL, both of which are wildtype strains.

Noncomplementation Screen and Identification of Mutants

Mutagenized G0 males were crossed to $ast^{ti272z/ti272z}$; $Tg(Brn3c:gap43\text{-}GFP)^{s356t}$ or $Tg(Isl2b:GFP)^{zc7}$ females and the F1 progeny were screened for any retinal pathfinding errors at 4 or 5 dpf under a dissecting scope using GFP fluorescence. Some of these crossings were performed with natural matings, but most were produced by in vitro fertilization. Any embryos with pathfinding errors were individually raised with daily water changes until placed on our main fish system at 3 weeks of age. We tried several

different foods including powders and rotifers, but had the best success feeding with live paramecia until larvae were 3 weeks old and large enough to eat live brine shrimp.

Adult F1 mutants were crossed to both wildtype and *ast* $^{ti272z/ti272z}$ fish for complementation testing and to propagate the mutation. To distinguish between *ti272z* and new alleles of *astray*, we performed allele-specific PCR. We placed fin-clips in lysis buffer (2mg/mL proteinase K, 50mM Tris pH 8.3, 100 mM NaCl, 0.2% SDS, and 5 mM EDTA) to digest overnight at 55°C then inactivated the proteinase K at 95°C for 10 minutes. We then ran 2 PCRs for each sample using either *ti272z* (GAATGACTCCTCGTCGCTCT and CAGCTCCTTTTGCACATGTT**A**) or wt (GAATGACTCCTCGTCGCTCT and CAGCTCCTTTTGCACATGTT**T**) allele-specific primers. (The last base in bold represents the specific mutation of the *ti272z* allele.) Each PCR used multiplexed *netrin1a* specific primers (ACCATTCAGAGCTGGACAGAA and ATGTATCTGAAACGTGACGCC) as a control.

Eight-Point Scoring and Temperature-Sensitive Scoring

To quantify the *astray* phenotype we devised an eight-point scoring system modified from that used in Pittman et al., 2008. Embryos were individually scored for eight different mistakes: A) extra crossings at the posterior commissure; B) extra midline crossings near the habenular commissure; axons erroneously wandering in the C) left and D) right diencephalons; E) left and F) right caudal projections; and G) left and H) right anterior projections. The average number of errors made for a clutch was the eight-point score for that allele. This scoring system also revealed which mistakes are most common.

With a means of quantifying the phenotype in place, we could determine whether any alleles are temperature sensitive (ts); some of the original F1 mutants were raised at 33°C in the hope of isolating ts alleles. To test for differences in phenotypic strength due to changes in temperature, we compared eight-point scores for each candidate allele raised at 23°C and 33°C starting at 1 dpf (having raised all embryos at 28.5°C for the first 24 hpf). We used the null allele *ti272z* as a reference point for the two temperatures. To account for the different rates of development at these temperatures, we scored at 3 dpf for 33°C and 5 dpf for 23°C, in contrast to the 4 dpf for 28.5°C. These regimens lead to approximately equivalent developmental stages in wildtype fish (Kimmel et al., 1995).

Whole Eye Fills

To better understand the "empty tectum" phenotype, we labeled the projection from each eye in fixed embryos by injecting DiI and DiO dissolved in chloroform (Fricke et al., 2001).

In Situ Hybridization

To test for differences in mRNA expression of *astray*, we performed in situ hybridizations with a *robo2* probe as previously described (Lee et al., 2001). Embryos at dpf were scored for the *astray* phenotype by use of the *Tg(Brn3c:gap43-GFP)^{s356t}* transgene and mutants were tail-clipped so that in situs could be performed on both mutants and wildtype siblings under identical conditions.

RT-PCR Sequencing

To determine the molecular nature of the new *astray* mutations, we performed RT-PCR. We identifed homozygotes based on their retinotectal phenotype at 4 dpf and triturated them in Trizol (Invitrogen 15596-026) before storing at -80°C. Each Trizol sample was chloroform-extracted and precipitated with isopropanol, resuspended by adding 350uL of RLT buffer (Qiagen RNeasy Mini kit), and processed with the RNeasy protocol.

Reverse transcription was performed using 1μg of RNA and the Superscript protocol (Invitrogen 18080-051), using a mixture of random hexamers and oligo dT primers. cDNA was amplified in five overlapping regions of approximately 1 kb each (Table 3.1). PCR products were gel-purified and directly sequenced using each of the original amplification primers. Sequence data were trimmed, combined and analyzed using Sequencher software (Gene Codes Corporation).

Results

Screen Design

The zebrafish visual pathway is ideal for investigating Robo2 signaling. This system provides powerful genetics and has a plethora of established protocols and reagents. The visual pathway is very well characterized and easy to visualize even under a dissecting scope, eliminating the need for cumbersome mounting. Also, even though

Table 3.1. List of PCR and Sequencing Primers Used for Amplifying and Sequencing the New *robo2* Alleles. The coding region was divided into five overlapping segments of about 1kb each. Also shown are the splice form specific primers and some internal primers.

Robo2 Segment	Primer Name	Primer Sequence
1	CF10F	AGAAACGTGTTCTGGGGTTG
1	KR13	TGACCTCAAGCTGTGCTTTG
2	CBC2F	TCCTGTTTCCAAATCAACCC
2	KR15	CGTCCATGTGACCTGTATGG
3	KR14	TCAGCCAATCAGTGAGCAAC
3	311-T7F4	TGAGCACTGGGCATCACATCT
4	311-1-T3F3	GGCCTGCTGGGTCATTCTGAT
4	KR17	CCTAATTGGTGGCGACATCT
5	KR16	TTTCCTTTGGCAAACAGTCC
5	CF6R	GTGGGTTGCATGTCCATCTT
exon 7	KR29	CATGGTCGGCGAAAGAGACA
exon 7	KR30	ACTGCGGTGCAGCGACAGGG
exon 19	KR31	GGAACGTCACTGCAGGGGTG
exon 23	KR32	GCAATAACACACTCCTTTTC
exon 2	KR33	CTCCTGCAATAACACACTCC
exon 23	KR34	CCACCTTTTCCACCTGACAG
internal	KR35	CATCTCCTGGGACCCTCCGC
internal	CF5F	CCGTGGAGTGGTACAAGGAT
internal	CBC1R	ACATCTGTAGGGTTCTGCCG
internal	CF1R	GACCCTGCCGGATGATG

there are multiple Robos in fish, Robo2 is the only one expressed by retinal ganglion cells (RGCs) so that genetic redundancy should not pose a problem (Lee et al., 2001).

To give us better insight into the signaling pathway of the Robo2 receptor, we designed a screen for mutations that fail to complement *astray*. Such a screen could in principle yield two classes of noncomplementing mutations: allelic or nonallelic. Allelic mutations would be new mutations in the *astray* gene, failing to complement because they interfere directly with Robo2 function. Nonallelic mutations would be mutations in other genes that, when present heterozygously, cause the amount of Robo2 signaling to be reduced below a threshold required for normal axon pathfinding. There are several examples of nonallelic noncomplementation, including several that affect Robo signaling in *Drosophila* (For example: Bashaw et al., 2000; Fan et al., 2003; Hu et al., 2005).

In designing this screen, we took advantage of two signature features of *astray* mutants – they are fully homozygous viable and fertile. While these mutants are morphologically normal, retinal axons make drastic pathfinding errors that can be visualized in live larvae using GFP transgenes. Since *ti272z* is a fully penetrant null allele, a *ti272z*/+ background should reduce gene function significantly, increasing the chance of detecting noncomplementation mutants. Also, this allele is fully recessive, which should minimize false positives. These features allowed us to screen F1 larvae, each of which carried an independently mutagenized genome, testing many more mutagenized haploid genomes than would be possible in a traditional F3 screen. In fact, we were able to screen tens of thousands of genomes - numbers that would otherwise be completely impractical. To my knowledge, this is the largest genetic screen ever performed in a vertebrate.

During the latter part of the screen, we altered rearing conditions to try to detect temperature sensitive (ts) alleles. A ts mutation would provide a valuable means to switch Robo2 signaling on and off by simply changing the rearing temperature. Most F1 clutches were raised at a higher, nonpermissive temperature of 33°C starting at 24 hours post fertilization (hpf), until screening. Starting at 24 hpf avoided possible problems with early development caused by the higher temperature; note that the first axons do not leave the eye until 30 hpf. The Robo family of receptors, including Astray, contain several immunoglobulin (IG) domains (Figure 3.1) and alterations in IG domains have been known to produce ts mutations. Indeed, ts mutations have been found in the *C. elegans* homolog of *robo*, *sax-3* (Zallen et al., 1998).

Overview of Noncomplementation Screening

To generate mutations, wildtype AB males were mutagenized with ENU. ENU was chosen as a mutagen because it preferentially generates single base changes rather than other types of mutations such as inversions and deletions (Guttenplan, 1990). We reasoned that single base mutations would be more likely to generate missense mutations that might lead to nonallelic noncomplementation or ts mutations.

The screening employed several independent batches of mutagenized G0 males. These G0 males should bear many independent mutations in their spermatogonia, and generate progeny that are heterozygous for mutations in many different genes. This was confirmed by performing a specific locus test, crossing G0 males to *golden* testers. All batches of mutagenized G0s yielded *golden* mutations. The final batch of G0s used gave

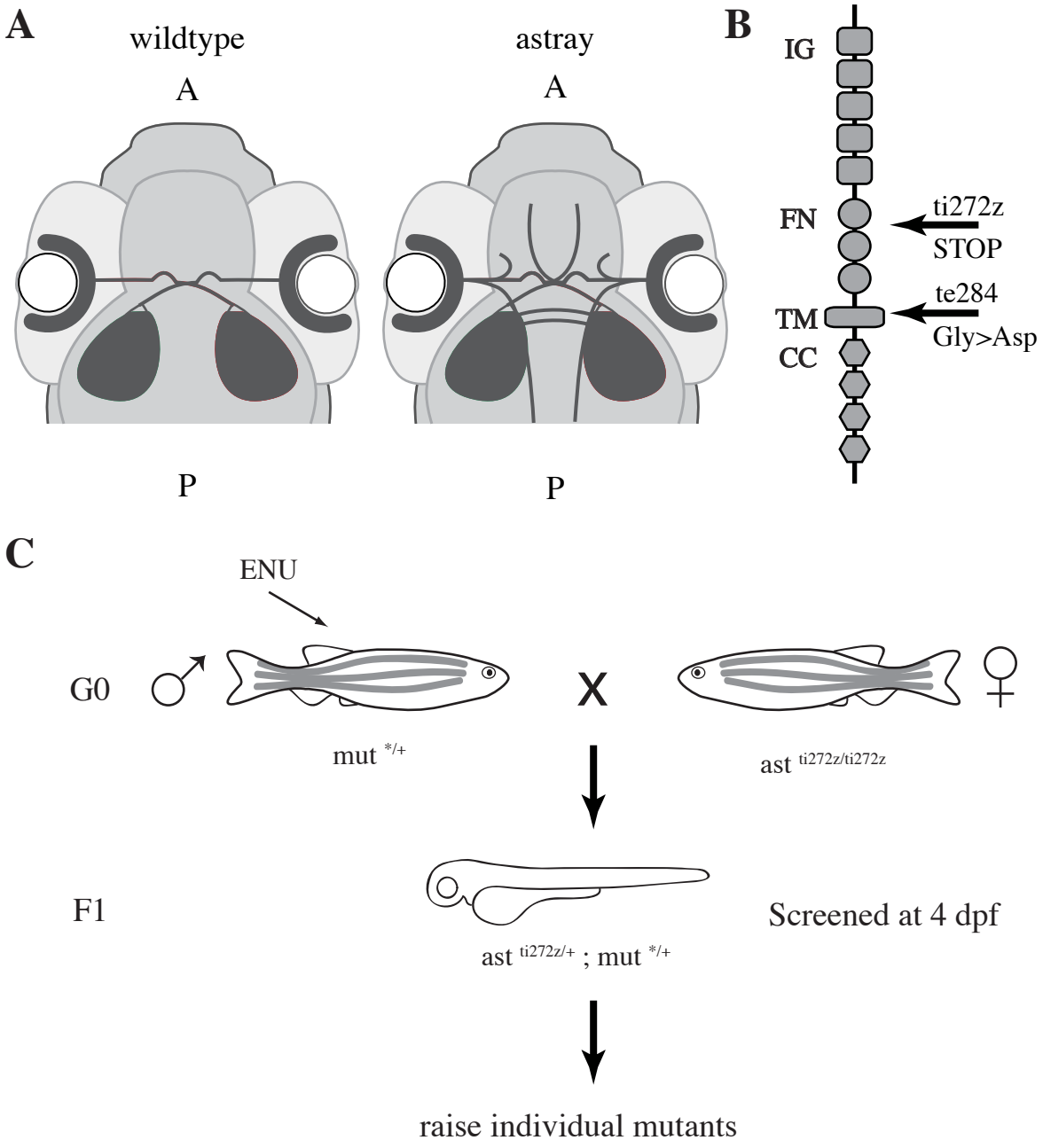

Figure 3.1 Astray Signaling in Retinal Pathfinding and Screen Design. (A) dorsal views (A, anterior; P, posterior) illustrating the retinal projection in wildtype and astray embryos. Note the many errors seen for astray throughout the pathway. (B) The structure of the Robo2 receptor showing the immunoglobulin (IG), fibronectin (FN), transmembrane (TM), and conserved cytoplasmic (CC) domains. Also shown are the nature of the mutations for the *ti272z* and *te284* alleles. (C) Noncomplementation screen design that allows screening at the F1 level.

8 *golden* embryos out of 3710, for a rate of 1 *golden* allele in 464 haploid genomes, while earlier batches gave rates of 1 in 600-800.

Mutagenized G0 males were crossed to female *ast*$^{ti272z/ti272z}$*; Tg(Brn3c:gap43-GFP*$^{)s356t}$ /+ testers (Figure 3.1). This transgene labels the retinotectal projection and allowed us to screen the live F1 progeny relatively quickly under a dissecting scope at 4 to 5 dpf (Xiao et al., 2005). One drawback is that the *Tg(Brn3c:gap43-GFP*$^{)s356t}$ transgene is very difficult to homozygose, so that usually only half of the F1 progeny were informative. Screening was repeated weekly for 79 weeks, allowing us to screen 21,649 haploid genomes (Table 3.2). We isolated F1 progeny that demonstrated retinal axon guidance errors, and attempted to raise them to recover the mutation. Of the 21,649 F1 larvae screened, we identified 42 that had errors in retinal pathfinding, giving a rate of 1 pathfinding mutant per 515 F1s. Of these 42 larvae, 15 had gross morphological defects that precluded survival, such as heart edema or an uninflated swim bladder. These defects presumably reflect cumulative deleterious mutations, or dominant mutations in genes essential for proper patterning. The raising of individual mutant fry proved more difficult than originally expected, and no mutant fry survived for the first half of the screen. At this point we improved our fish care, particularly in feeding and water quality, and had noticeably increased success in fry-raising. During the second half of the screen, with our improved fry-raising protocol, 12 out of 15 healthy-looking embryos were successfully raised to adulthood.

The second half of the screen used *Tg(Isl2b:GFP*$^{)zc7}$ tester females in addition to *Tg(Brn3c:gap43-GFP*$^{)s356t}$ (Table 3.2). *Tg(Isl2b:GFP*$^{)zc7}$ larvae express GFP earlier and more brightly than *Tg(Brn3c:gap43-GFP*$^{)s356t}$ larvae, and have the advantage that the

Table 3.2 Screen Summary. The screen was conducted weekly for 79 weeks, representing 21,649 haploid genomes screened. 4,742 of the F1 larvae were raised at a higher temperature to potentially recover temperature sensitive mutations. During the latter half of screening, an improved fry raising protocol allowed us to better raise individual fry. 42 embryos with retinal pathfinding defects were identified, including 27 that were otherwise morphologically normal. Of these, 12 were successfully raised to adulthood.

Total haploid genomes screened	21,649
Screened at 28.5°C	16,907
Screened at 33°C	4,742
Screened using the Brn3c:GFP transgene	20,350
Screened using the Isl2b:GFP transgene	1,299
Total pathfinding mutants observed (1 per 515 F1)	42
Mutants with gross defects, not raised	15
Relatively healthy looking mutants	27
Raised with old feeding protocol	12
Raised with new feeding protocol	15
Number of mutants raised to adulthood	12
Sterile mutants	3
Mutants which bred	9

transgene can be homozygosed so that every F1 embryo is informative (Pittman et al., 2008).

Another feature added partway through the screen was the raising of some of the F1 fry at a higher, presumably nonpermissive temperature (33°C) in order to recover potential ts alleles. Three of the mutants were so raised: *zc16*, *zc17* and *zc26* (Table 3.3).

Mutants Recovered From the Screen

Of the 12 pathfinding mutants that were raised to adulthood, 9 bred successfully. All were female, as is often seen when fish are raised at low density. One drawback of screening at the F1 level is that we must be able to raise and breed every F1 fish to recover the mutation. With the improved rearing protocol, we obtained 9 fertile adults out of 15 adults which is quite a good yield, especially given the mutational load carried by these animals.

To test whether each mutant represented allelic or nonallelic noncomplementation we crossed the F1 mutant to both wildtype and *astray* fish. The cross to wildtype distinguishes between $ast^{ti272z/mut}$ and $mut^{*/+}; ast^{ti272z/+}$. If the new mutation is allelic with *astray*, this is simply an outcross and the resulting progeny will all be heterozygous for *astray* and phenotypically wildtype. For a nonallelic mutant, outcrossing will generate four genotypes, including the double heterozygote that will be phenotypically *astray* (Figure 3.2). All F1s tested generated only wildtype progeny when crossed to wildtype (Table 3.3), showing that the new alleles are all either *astray* alleles, or very closely linked to *astray* on LG15.

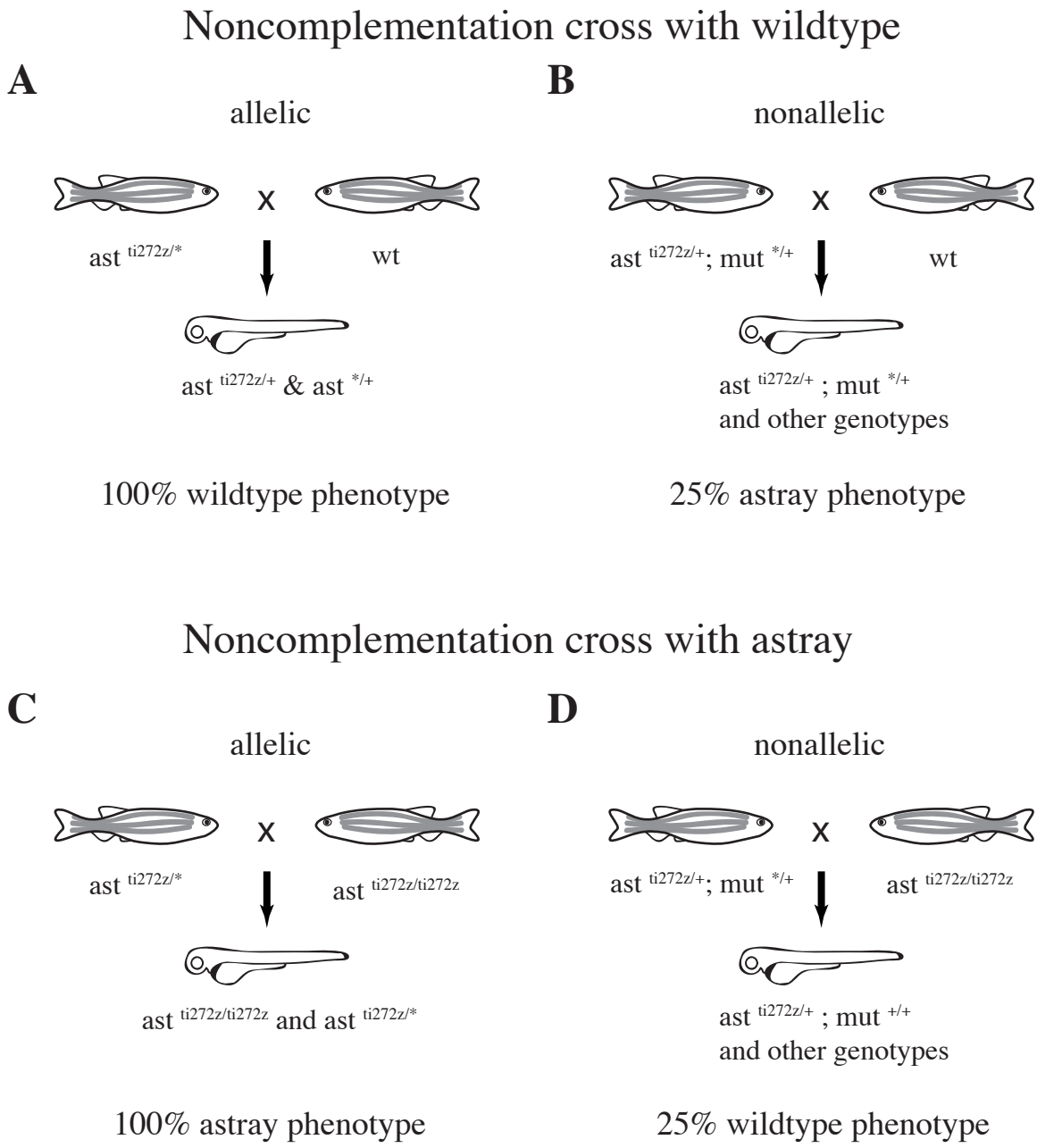

Figure 3.2 Noncomplementation Tests. Noncomplementation crosses with wildtype for both allelic (A) and nonallelic (B) cases of mutations. The presence of astray embryos indicates nonallelic noncomplementation. Noncomplementation crosses with astray for both allelic (C) and nonallelic (D) mutants. The presence of wildtype progeny would indicate that the mutations is nonallelic with *astray*.

Table 3.3 Summary of *astray* Alleles. The numbers of wildtypes from crosses to wildtype and *astray* demonstrate that all mutations are allelic with *astray*. The nature of each mutation is shown where known. *zc9*, *zc10*, *zc13*, and *zc17* had no mutations in their coding sequence. The domain containing each mutation is shown, including immunoglobulin (IG), fibronectin (FN), and transmembrane (TM) domains. The eight-point score is a measure of the phenotypic strength for each allele with a known null allele, *ti272z*, having a score of 5.64 ±1.30. The eight-point score for *zc14* was actually scored over the C7 deletion. Both *zc13* and *zc19* sometimes show the "empty tecta" phenoype. *zc16*, *zc17*, and *zc26* were raised at 33°C and are potentially temperature sensitive.

Allele name	wt from cross w/ wt	wt from cross w/ *ast*	Sequence change	Amino acid change	Location	Eight-point score (n) ± std dev	Notes
zc9	73/73	0/19				4.04 (48)±1.31	
zc10	19/19	0/48				1.65 (92)±1.10	
zc11	149/149	0/115	G526A	Ser>asp	IG1/IG2	5.63 (46)±1.18	
zc13	175/175	0/116				2.51 (59)±1.83	empty tecta
zc14	206/206	0/61	16bp ins.	frameshift	IG1/IG2	6.27 (55)±1.25	*zc14/c7*
zc16	84/84	0/96	C1678A	stop	IG5/FN1	5.73 (33)±1.48	tested at 33°
zc17	72/72	0/83				6.08 (25)±1.08	tested at 33°
zc19	80/80	0/116	T1609A	Ile>Asn	IG5	1.21 (63)±1.50	empty tecta
zc26	153/153	0/57	A1767T	Gln>Leu	FN1	5.40 (72)±1.41	tested at 33°
te284			G2812A	Gly>Asp	TM	2.80 (35)±1.57	
te378			C304A	Pro>Gln	IG1	3.55 (135)±1.33	
ti272z			A2070T	stop	FN1/FN2	5.64 (178)±1.30	

The second noncomplementation test was to cross the F1 to *ti272z* homozygotes. If the new mutation is allelic with *astray*, this is simply an incross and all the resulting progeny will be *astray*. For a nonallelic mutant, however, crossing to *astray* homozygotes will yield some $ast^{ti272z/+}$; $mut^{+/+}$ progeny that would be phenotypically wildtype (Figure 3.2). All F1s generated only *astray* progeny, again indicating that they are all mutations in *astray* or else closely linked genes (Table 3.3). Although we had hoped to find mutations in both *astray* and new genes, new alleles of *astray* are potentially informative in revealing mutations in specific domains that could be valuable in understanding interactions with other proteins. We were pleased, and somewhat surprised, at the lack of false positives in the screen: none of the F1s raised to adulthood and bred failed to yield offspring with retinal pathfinding defects.

Characterization of Mutant Alleles

To recover the new mutations, mutants were outcrossed to wildtype. F2 carriers of the new alleles were distinguished from *ti272z* carriers using allele specific PCR, then incrossed to obtain F3 homozygous animals. All of the new mutant alleles are recessive to wildtype. We then incrossed homozygotes to determine the penetrance of each allele. The only allele that is not fully penetrant is *zc19*, which is only 30% penetrant. All other alleles yielded 100% of homozygous larvae with detectable retinotectal errors.

To characterize the strength of each allele, we devised a semi-quantitative score of the *astray* phenotype. We chose eight canonical errors that are most often seen in *astray* mutants (Pittman et al., 2008). These are A) extra crossings at the posterior commissure; B) extra midline crossings near the habenular commissure; axons

erroneously wandering in the C) left and D) right diencephalon; E) left and F) right caudal projections; and G) left and H) right anterior projections (Figure 3.3). Using the *Tg(Brn3c:gap43-GFP)s356t* transgene to illuminate the retinal pathway, an individual embryo can be scored for each of these eight classes of errors, and given a score representing the total number of error classes made. This score ranges from 0 (wildtype) to 8 (an individual which made every class of error). Although the score for individuals may vary considerably, the averaged score for a given allele is quite consistent. For example, the strong *zc17* allele shows 6.08 ±1.08 errors on average (Table 3.3), although individual *zc17* embryos vary considerably in their phenotype (Figure 3.3).

To demonstrate the reproducibility of this eight-point scoring method, several clutches of *ti272z* embryos were scored, including clutches obtained from a single tank of fish and also from a distantly related tank. All clutches scored gave very similar results, indicating that the frequency of each error class is relatively consistent (Figure 3.3). They also all make similar total numbers of mistakes, 5.7 on average. The cumulative histogram of scores further demonstrates that the eight-point scoring method is a reproducible means of quantifying phenotypic strength (Figure 3.3).

Each new allele was analyzed by this eight-point scoring method to determine its relative phenotypic strength (Figures 3.4 and 3.5). Five alleles - *zc11*, *zc14*, *zc16*, *zc17*, and *zc26* - have a strong phenotype similar to the null allele *ti272z*, and we consider them null. *zc9, zc10, zc13*, and *zc19*, have weak or intermediate phenotypic strengths, as do *te284*and *te378*, two of the other alleles identified in the original Tübingen screen (Trowe et al., 1996; Karlstrom et al., 1996).

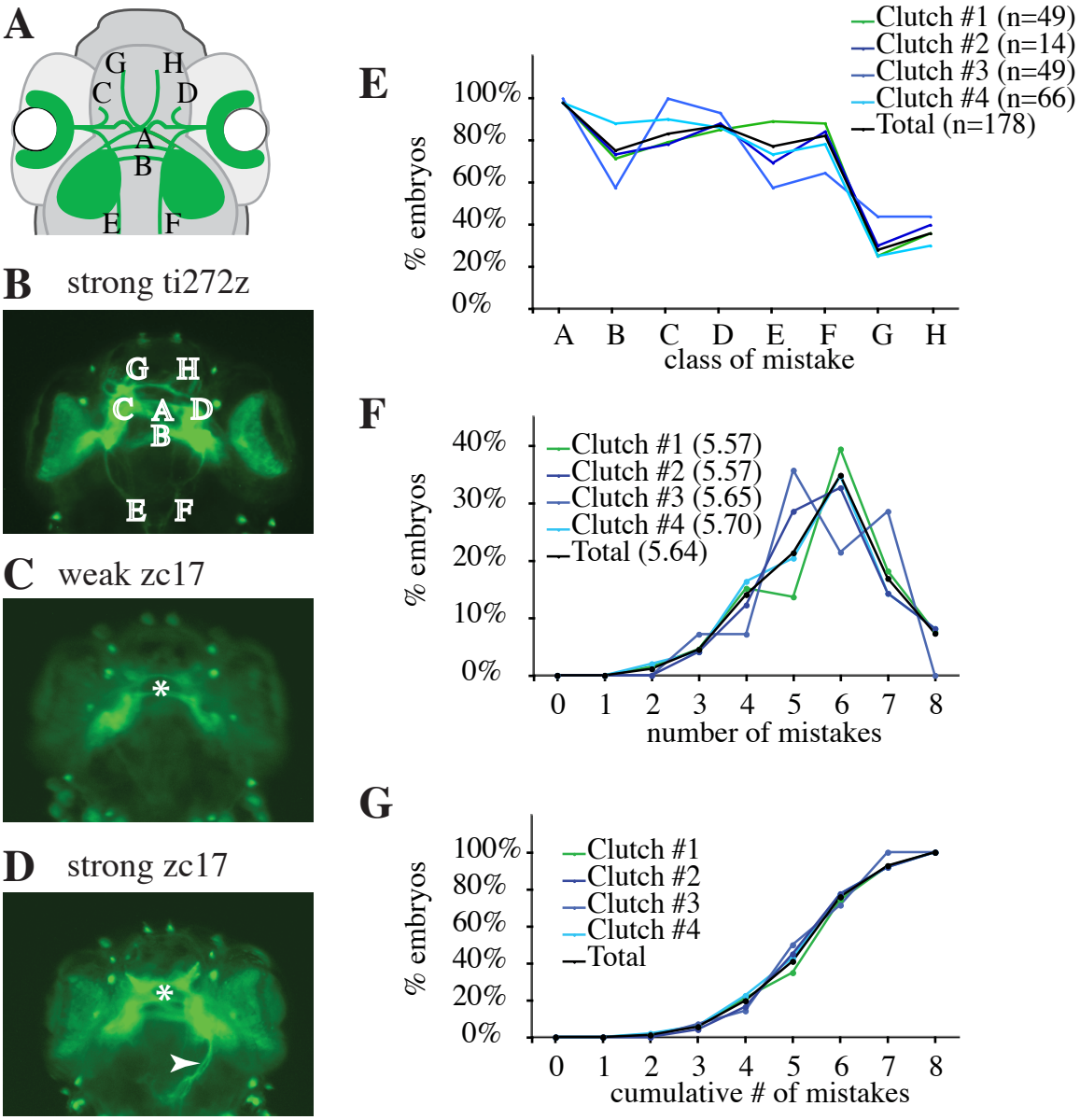

Figure 3.3 Eight-Point Scoring of ti272z. (A) Diagram and (B) micrograph showing each of the 8 classes of errors: extra midline crossings at the A) posterior or B) habenular commissure; errors in the C) left and D) right diencephalon; E) left and F) right caudal projections; and G) left and H) right anterior projections. Isolated spots are neuromasts, which are also labelled by the brn3c:GFP transgene. (C-D) Weak and strong examples demonstrating the variability of the *zc17* allele. Extra crossings at the midline (asterisks) are very common but other mistakes such as caudal projections (arrowhead) are seen in fewer embryos. (B-D) Dorsal views using fluorescent stereomicroscope. (E) Frequencies of each class of mistake for the *ti272z* allele. Four individual clutches are shown, as well as the total of all clutches. (F) Histogram of the number of mistakes showing the 8-point score of each clutch in parentheses. (G) Cumulative histogram for the *ti272z* allele.

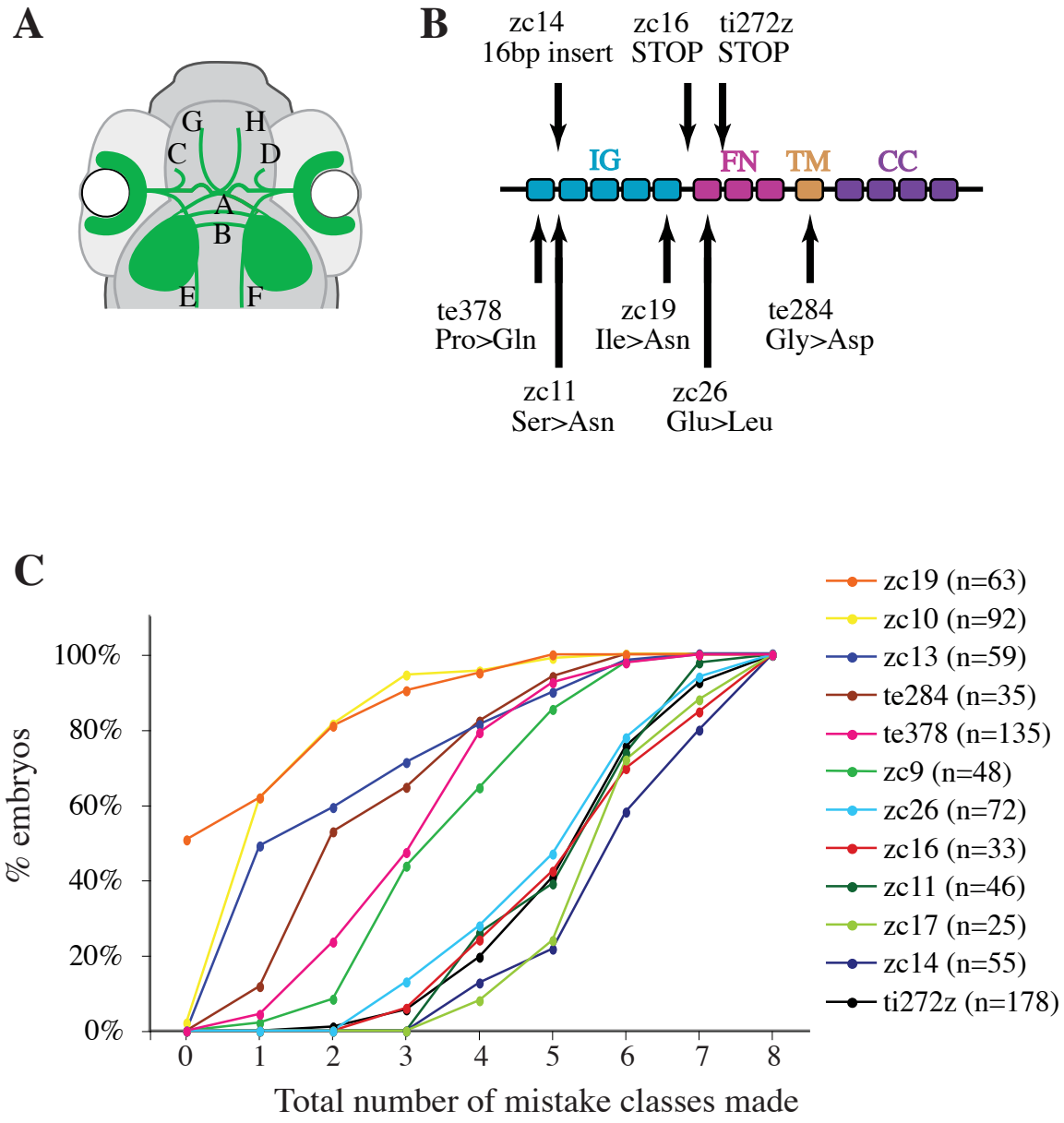

Figure 3.4 Eight-Point Scoring of Alleles. (A) Diagram of the 8 classes of mistakes made by astray. (B) The structure of Astray showing immunoglobulin (IG), fibronectin (FN), transmembrane (TM), and conserved cytoplasmic (CC) domains. The locations of known mutations are also indicated. (C) Cumulative histogram showing the distribution of phenotypic strengths of astray alleles. The *zc14* allele is scored over the C7 deletion not as *zc14* homozygotes.

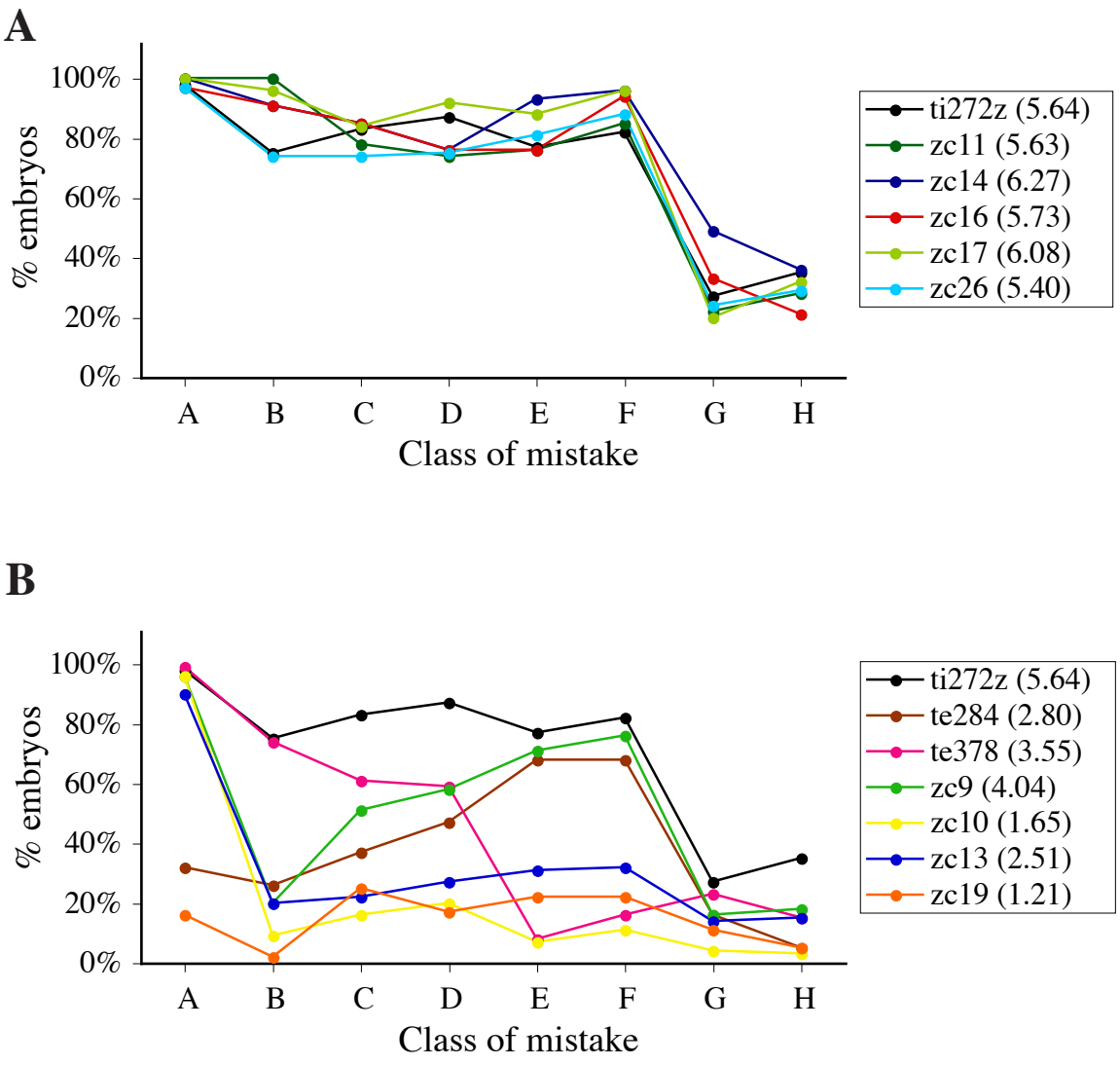

Figure 3.5 Graphs for Each Allele Showing the Distribution of Errors Made. (A) shows the strong (presumably null) alleles and (B) shows the hypomorphic alleles. *ti272z* is shown in black at the top of each column for a reference of a null allele. Also shown is the 8-point score for each allele as a measure of overall phenotypic strength. The *zc14* allele is scored over the C7 deletion.

Temperature Sensitivity

During the screen, some F1 larvae were raised at 33°C, in hope of obtaining temperature sensitive (ts) alleles. Three of the mutants, *zc16*, *zc17* and *zc26,* were so raised, although the phenotypic strength and nature of the mutation for *zc16* and *zc26* make them poor ts candidates as their function is unlikely to be restored by stabilizing protein confirmation from shifting to a lowered temperature. To test whether they were ts, we measured eight-point scores at 23°C and 33°C, in addition to the 28.5°C originally used for scoring. The embryos were temperatur-shifted after 24 hpf to remove the possibility of temperature extremes causing early developmental defects. We reasoned that a difference of 10°C might be sufficient to induce changes in protein conformation and affect Robo2 function. As controls, we also scored *ti272z* and *te284* at the additional temperatures. Temperature is well known to affect the rate of development (Kimmel et al., 1995). We found that raising embryos to 24 hpf at 28.5°C, then to 5 dpf at 23°C was comparable in developmental time to 4 dpf at 28.5°C. Although embryos raised to 24 hpf at 28.5°C, then to 3 dpf at 33°C were comparable to 4 dpf at 28.5°C, we obtained more consistent results by scoring at 4 dpf at 33°C (roughly comparable to 5 dpf at 28.5°C). For all alleles tested, the total number of mistakes was very similar across the three temperatures. However, the specific types of mistakes seemed to change slightly at different temperatures (Figure 3.6). For example, the *zc17* allele does not make many anterior projections (G and H) at 33°C, although it does at both 23°C and 28.5°C.

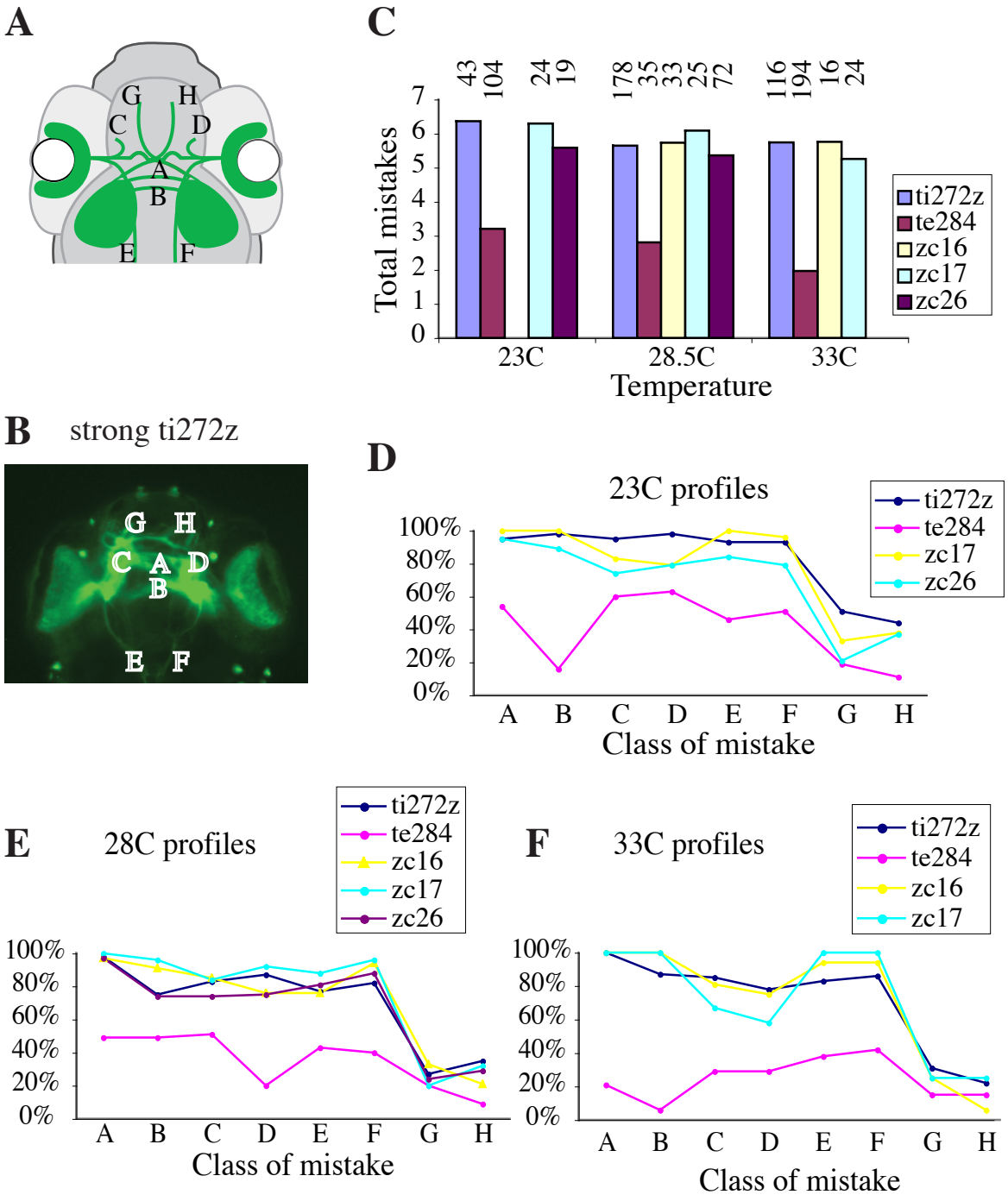

Figure 3.6 Temperature Sensitive 8-Point Scoring of *astray* Alleles. (A) Diagram and (B) micrograph showing each of the 8 classes of errors. (C) Graph showing that none of the alleles tested show any change in total number of mistakes made at different temperatures. Profiles of *astray* alleles at (D) 23ºC, (E) 28ºC, and (F) 33ºC.

"Empty Tectum" Phenotype

One unusual phenotype observed in alleles *zc13* and *zc19* was the complete failure to innervate one or both tecta even when none of the eight canonical pathfinding errors were made (Figure 3.7). Strong *astray* phenotypes occasionally display a weakly innervated tectum because many axons misroute before reaching the tectum; however, in *zc13* and *zc19*, "empty tecta" can occur even when no misrouted axons are evident. It is interesting to note that both of these alleles are phenotypically weak (eight-point scores of 2.51 ±1.83 and 1.21 ±1.50 respectively). This "empty tectum" phenotype has not been observed in the four original alleles of *astray*, including *te284* or *ti272z*. There are two possible explanations for this observed phenotype. The first is a retino-retinal projection, in which all the axons from one eye project into the contralateral eye. The second is that all the axons from one eye project to the ipsilateral tectum, as seen in the *belladonna* mutant (Seth et al., 2006).

To distinguish between these possibilities, we used the lipophilic dyes DiI and DiO to label separately the axons from each eye (Fricke et al., 2001). Embryos that displayed one or both "empty tecta" were identified by the *Tg(Brn3c:gap43-GFP)s356t* transgene and fixed with PFA, Then the left eye was injected with DiI and the right eye with DiO. All of the embryos analyzed for both *zc13* (n=6) and *zc19* (n=3) demonstrated only retino-retinal projections (Figure 3.7). Neither allele demonstrated any projections to the ipsilateral tectum. Thus, it appears that when Robo2 function is only partially reduced, the separation between optic nerves can become abrogated so that axons from one eye enter the contralateral optic nerve and follow it back into the other eye.

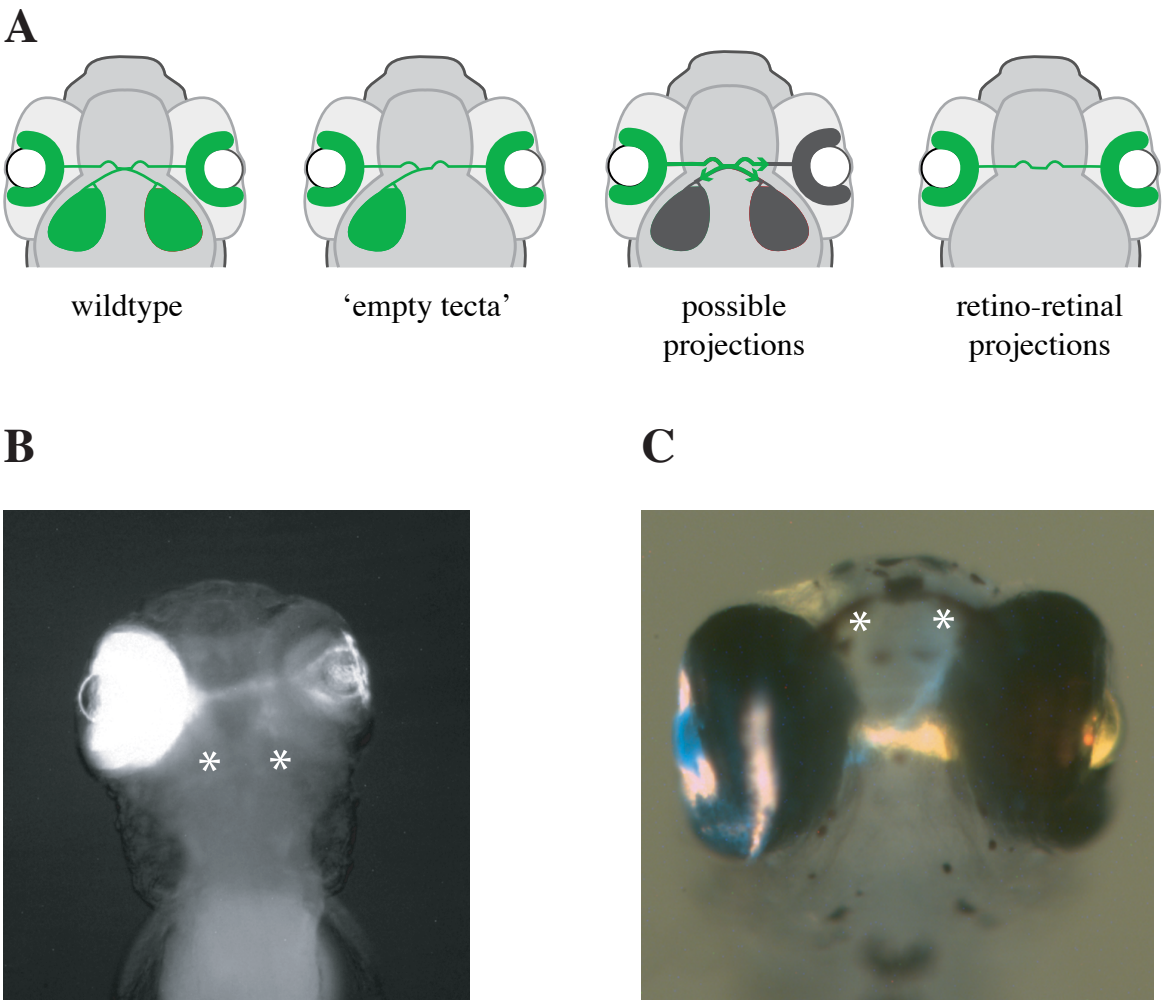

Figure 3.7 The 'Empty Tecta' Phenotype Results From Retino-Retinal Projections in Both *zc13* and *zc19* Mutants. (A) Diagram showing the projections made in both wildtype and 'empty tecta' embryos. Axons could be taking several different paths at the optic chiasm including towards the ipsilateral eye or either optic tectum. Also shown is the retino-retinal projection that is observed in both *zc13* and *zc19* mutants. (B) A dorsal view showing the retino-retinal projection of *zc19* a embryo. (C) A head on view showing these projections in a *zc13* embryo. The eye on the left projects normally in a dorsal direction toward the contralateral optic tectum after leaving the optic chiasm (blue). However, axons from the eye on the right project into the contralateral eye (yellow). Asterisks indicate locations of tecta.

Identification of Molecular Lesions

Once all the mutants had been identified as *astray* alleles, we set out to determine the molecular nature of each mutation. F3 or F4 homozygote larvae from each allele, identified by retinal pathfinding errors, were pooled and used for RT-PCR. The coding region of the *astray* gene was divided into five slightly overlapping segments of approximately 1kb and primer pairs were designed for each (Table 3.1).

Several common polymorphisms found in multiple alleles were identified and subsequently ignored. Only changes resulting in differences at the amino acid level were considered significant. One issue that complicated the initial sequencing was alternative splicing in the *astray* locus. Three exons are employed alternately; in these cases splice form specific primers were designed to amplify the sequence. Mutations were identified for five alleles.

zc14 is a 16bp insert after the first immunoglobulin (IG) domain that leads to an early stop codon. The first two IG domains have been implicated in Slit binding (Sundaresan et al., 2004). z*c16* encodes a nonsense mutation between the last IG domain and the first fibronectin (FN) domain. z*c14* and *zc16* should lead to truncated proteins like *ti272z* whose mRNAs would likely be targets of nonsense mediated decay. z*c11* causes a conserved serine to become asparagine between the first two IG domains. *zc26* is a isoleucine to asparagine missense mutation in the first FN domain. z*c19* encodes a missense mutation changing a glutamine to a leucine in the last IG domain. All of the point mutations (*te378, zc11, zc19*, and *zc26*) are in residues that are conserved in zebrafish, mouse, and human Robo2.

In Situ Analysis

Four of the alleles showed no coding changes in their sequence. We reasoned that their phenotypes could be due to a change in *astray* expression. We performed in situ hybridization experiments on three of the alleles to test this hypothesis. Clutches of PFA fixed embryos containing both homozygous and heterozygous animals were scored for phenotype by visualizing the retinal pathway with the *Tg(Brn3c:gap43-GFP)s356t* transgene. Homozygotes were marked by clipping their tails, and processed for in situ hybridization in the same tube as their siblings. We used the *ti272z* allele as a positive control and saw a noticeable reduction in expression of *astray* $^{ti272z/ti272z}$ compared to *astray* $^{ti272z/+}$.

In situs on the *zc10* allele did not reveal any detectable changes in expression between mutants and wildtype embryos in the brain or retina (Figure 3.8). This allele is one of the weakest phenotypically and it may be that any difference in expression is too subtle to detect reliably by in situ hybridization (Table 3.3).

In situs on the *zc9* allele showed a potential slight reduction in Robo2 expression in the retina (Figure 3.8). The *zc9* allele is intermediate in terms of phenotypic strengths (Table 3.3).

The *zc17* allele is phenotypically null (Table 3.3) and in situs showed a reduction of Robo2 expression, particularly in the forebrain (Figure 3.8). This allele may have a mutation in a regulatory region, such as in the promoter that reduces the expression of Robo2 and thus reduces its function.

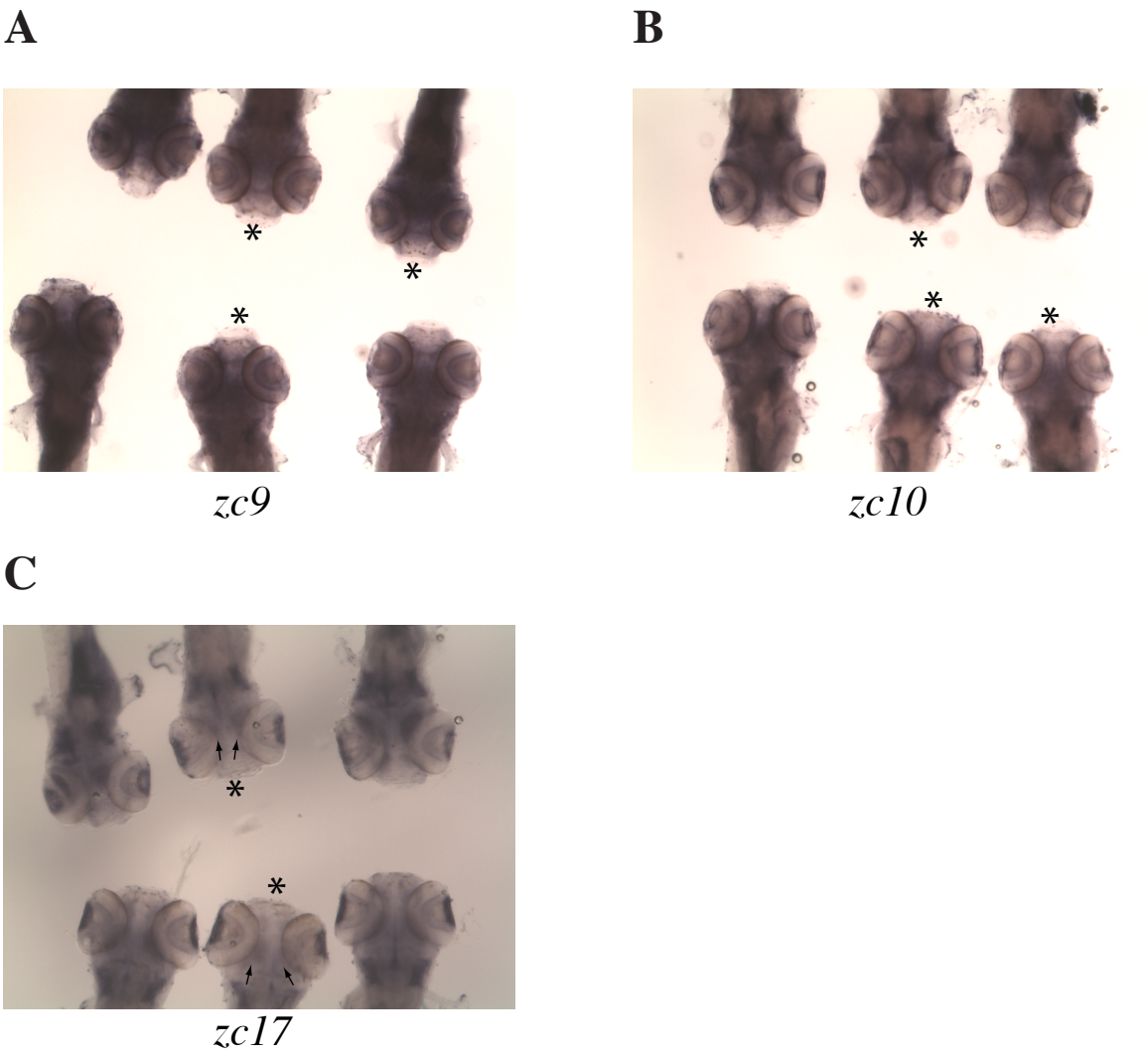

Figure 3.8 In Situ Hybridizations for *robo2* Expression of the *zc9*, *zc10*, and *zc17* Alleles. Each image shows dorsal views of both mutants (marked by asterisks) and wildtype siblings that were processed for in situ hybridization under identical conditions. (A) There were no detectable differences between the *zc9* allele and wildtype. (B) The *zc10* allele had a subtle reduction of *robo2* expression compared to wildtype. This is consistent with its intermediate phenotypic strength. (C) The *zc17* allele had the strongest reduction in *robo2* expression, consistent with its strong phenotype. The expression is particularly reduced in both the tecta (arrows) and the retina. All of these observations were confirmed by blind scoring.

Discussion

Phenotypes of New *astray* Alleles

The screen generated 12 mutants that were successfully raised to adulthood. Failure of three to successfully breed resulted in nine new alleles of *astray*. These alleles represent a wide variability of phenotypic strengths, including several that are similar to the previously identified null *ti272z* allele. This result in not surprising, since there are many possible molecular lesions that would completely remove the function of the Astray receptor. The presence of several phenotypically strong alleles gives us confirmation that we know the null phenotype.

The screen also recovered several hypomorphic alleles, including *zc10, zc13*, and *zc19*, which are weaker than the weakest previously-known allele, *te284*. Two of these, *zc13* and *zc19*, have the unusual phenotype of occasionally only innervating one of the optic tecta. This is due to retino-retinal projections to the contralateral eye. Although it is quite common in different *astray* alleles for some axons to project into the opposite eye, only these two alleles demonstrate completely uninnervated tecta, meaning that all the axons from one eye project into the opposite eye - even in a strong *ti272z* embryo some axons make it to both tecta. It seems that a critical level of Robo signaling is required at the optic chiasm to lead to the 'empty tecta' phenotype.

The screen was also designed to have the opportunity of recovering ts alleles. All of the three alleles that had this potential, *zc16*, *zc17*, and *zc26*, were phenotypically as strong as the null allele, *ti272z*. All three of these alleles were very similar to *ti272z* at all temperatures tested and so do not demonstrate any temperature sensitivity.

No Nonallelic Noncomplementation Mutants Identified

The objective of the screen was to obtain mutants that could further our understanding of Robo signaling. It was successful in generating new alleles of *astray*, but we also hoped to get mutations in other genes. Why did the screen not return mutants in any other genes? One possibility is that it did but that we were unsuccessful in raising them to adulthood. Although, the changes to fry raising for the second half of the screen improved our ability to raise individual fry, we cannot rule out the possibility of having lost a mutation in a new gene due to the F1 dying. Another possibility is that Robo signaling is not sufficiently reduced in *ti272z*/+ fish. In effect, the genetic background was insufficiently sensitized. Now that we have more alleles to choose from and a means of characterizing their phenotypic strengths, one could repeat the screen using different genotypes and possibly reduce Robo signaling more effectively.

The failure to recover *slit* mutants could well be due to genetic redundancy. Although recovering a mutation in *slit2* or *slit3* would be very useful, we suspected that this was unlikely due to the large overlap in their expression patterns. Redundancy could also be an issue with other potential interacting genes, especially since many genes in zebrafish have been duplicated.

Lastly, it could be that in zebrafish there are no genes that show nonallelic nonomplementation with *astray*. This is a bit unusual considering genes that interact with *robos* in *Drosophila* including: *abelson* and *enabled* (Bashaw et al., 2000); *dock* and *pack* (Fan et al., 2003); and *crGAP* (Hu et al., 2005). Nonallelic noncomplementation is unusual and the majority of genes do not demonstrate this phenomenon, even when they do interact (Yook et al., 2001).

The idea of the screen was motivated by the demonstration of several in *Drosophila* that show nonallelic noncomplementation with *robo*. Zebrafish seemed like an ideal choice for this screen since they only express one Robo family member in the visual system, *robo2,* and furthermore, *astray* mutants are homozygous viable. We decided that the advantage of being able to screen large numbers of genomes at the F1 level, outweighed the problem of having to raise individuals to recover any mutations. This approach resulted in a forward genetic screen with 21,649 haploid genomes screened – far more than any other vertebrate screen to date.

New Alleles Without a Known Coding Mutation

The screen generated several types of mutations including introduced stop codons, frameshifts, and missense mutations. All of the missense mutations are conserved across *robo2* genes in mouse and human. The lack of mutation in the coding region of some of the *zc9, zc10*, and *zc17* alleles led us to perform in situ hybridization to test if the level of Robo2 expression is reduced in these mutants. In situ hybridizations were not performed on the *zc13* allele due to its failure to breed. The result of the in situ hybridizations parallel the phenotypic strength of these alleles. *zc10* is a very weak allele (8 point score of 1.65 ±1.10) and there were no detectable changes in Robo2 expression. *zc9* is a medium-strength allele (8 point score of 4.04 ±1.31) and in situ hybridizations revealed a subtle reduction in Robo2 expression. The *zc17* allele is phenotypically null (8 point score of 6.08 ±1.08) and it had the strongest reduction in Robo2 expression, consistent with it having a strong phenotype.

It is also interesting to note that the screen only recovered mutations in the extracellular portion of the Robo2 receptor. The intracellular portion represents 41% of the coding region and contains 4 CC domains (Fricke et al., 2001). Although the intracellular region is less conserved overall than the extracellular region (Simpson et al., 2000), the introduction of a stop codon removing most or all of the CC domains should yield a receptor with no function. The fact that all identified mutations lie in the extracellular region suggests that it has more residues that are critical for Robo2 function.

References

Baier, H., S. Klostermann, T. Trowe, R. O. Karlstrom, C. Nusslein-Volhard and F. Bonhoeffer (1996). "Genetic dissection of the retinotectal projection." Development 123: 415-25.

Bashaw, G. J., T. Kidd, D. Murray, T. Pawson and C. S. Goodman (2000). "Repulsive axon guidance: Abelson and Enabled play opposing roles downstream of the roundabout receptor." Cell 101(7): 703-15.

Burrill, J. D. and S. S. Easter, Jr. (1995). "The first retinal axons and their microenvironment in zebrafish: cryptic pioneers and the pretract." J Neurosci 15(4): 2935-47.

Fan, X., J. P. Labrador, H. Hing and G. J. Bashaw (2003). "Slit stimulation recruits Dock and Pak to the roundabout receptor and increases Rac activity to regulate axon repulsion at the CNS midline." Neuron 40(1): 113-27.

Fricke, C., J. S. Lee, S. Geiger-Rudolph, F. Bonhoeffer and C. B. Chien (2001). "astray, a zebrafish roundabout homolog required for retinal axon guidance." Science 292(5516): 507-10.

Guttenplan, J. B. (1990). "Mutagenesis by N-nitroso compounds: relationships to DNA adducts, DNA repair, and mutational efficiencies." Mutat Res 233(1-2): 177-87.

Haffter, P., M. Granato, M. Brand, M. C. Mullins, M. Hammerschmidt, D. A. Kane, J. Odenthal, F. J. van Eeden, Y. J. Jiang, C. P. Heisenberg, R. N. Kelsh, M. Furutani-Seiki, E. Vogelsang, D. Beuchle, U. Schach, C. Fabian and C. Nusslein-Volhard (1996). "The identification of genes with unique and essential functions in the development of the zebrafish, Danio rerio." Development 123: 1-36.

Hu, H., M. Li, J. P. Labrador, J. McEwen, E. C. Lai, C. S. Goodman and G. J. Bashaw (2005). "Cross GTPase-activating protein (CrossGAP)/Vilse links the Roundabout receptor to Rac to regulate midline repulsion." Proc Natl Acad Sci U S A 102(12): 4613-8.

Karlstrom, R. O., T. Trowe, S. Klostermann, H. Baier, M. Brand, A. D. Crawford, B. Grunewald, P. Haffter, H. Hoffmann, S. U. Meyer, B. K. Muller, S. Richter, F. J. van Eeden, C. Nusslein-Volhard and F. Bonhoeffer (1996). "Zebrafish mutations affecting retinotectal axon pathfinding." Development 123: 427-38.

Kidd, T., K. Brose, K. J. Mitchell, R. D. Fetter, M. Tessier-Lavigne, C. S. Goodman and G. Tear (1998a). "Roundabout controls axon crossing of the CNS midline and defines a novel subfamily of evolutionarily conserved guidance receptors." Cell 92(2): 205-15.

Kidd, T., C. Russell, C. S. Goodman and G. Tear (1998b). "Dosage-sensitive and complementary functions of roundabout and commissureless control axon crossing of the CNS midline." Neuron 20(1): 25-33.

Kimmel, C. B., W. W. Ballard, S. R. Kimmel, B. Ullmann and T. F. Schilling (1995). "Stages of embryonic development of the zebrafish." Dev Dyn 203(3): 253-310.

Lee, J. S., R. Ray and C. B. Chien (2001). "Cloning and expression of three zebrafish roundabout homologs suggest roles in axon guidance and cell migration." Dev Dyn 221(2): 216-30.

Mullins, M. C., M. Hammerschmidt, P. Haffter and C. Nusslein-Volhard (1994). "Large-scale mutagenesis in the zebrafish: in search of genes controlling development in a vertebrate." Curr Biol 4(3): 189-202.

Pittman, A. J., M. Y. Law and C. B. Chien (2008). "Pathfinding in a large vertebrate axon tract: isotypic interactions guide retinotectal axons at multiple choice points." Development 135(17): 2865-71.

Rajagopalan, S., E. Nicolas, V. Vivancos, J. Berger and B. J. Dickson (2000a). "Crossing the midline: roles and regulation of Robo receptors." Neuron 28(3): 767-77.

Rajagopalan, S., V. Vivancos, E. Nicolas and B. J. Dickson (2000b). "Selecting a longitudinal pathway: Robo receptors specify the lateral position of axons in the Drosophila CNS." Cell 103(7): 1033-45.

Rothberg, J. M., D. A. Hartley, Z. Walther and S. Artavanis-Tsakonas (1988). "slit: an EGF-homologous locus of D. melanogaster involved in the development of the embryonic central nervous system." Cell 55(6): 1047-59.

Rothberg, J. M., J. R. Jacobs, C. S. Goodman and S. Artavanis-Tsakonas (1990). "slit: an extracellular protein necessary for development of midline glia and commissural

axon pathways contains both EGF and LRR domains." Genes Dev 4(12A): 2169-87.

Seeger, M., G. Tear, D. Ferres-Marco and C. S. Goodman (1993). "Mutations affecting growth cone guidance in Drosophila: genes necessary for guidance toward or away from the midline." Neuron 10(3): 409-26.

Seth, A., J. Culverwell, M. Walkowicz, S. Toro, J. M. Rick, S. C. Neuhauss, Z. M. Varga and R. O. Karlstrom (2006). "belladonna/(Ihx2) is required for neural patterning and midline axon guidance in the zebrafish forebrain." Development 133(4): 725-35.

Simpson, J. H., T. Kidd, K. S. Bland and C. S. Goodman (2000). "Short-range and long-range guidance by slit and its Robo receptors. Robo and Robo2 play distinct roles in midline guidance." Neuron 28(3): 753-66.

Solnica-Krezel, L., A. F. Schier and W. Driever (1994). "Efficient recovery of ENU-induced mutations from the zebrafish germline." Genetics 136(4): 1401-20.

Stuermer, C. A. (1988). "Retinotopic organization of the developing retinotectal projection in the zebrafish embryo." J Neurosci 8(12): 4513-30.

Sundaresan, V., E. Mambetisaeva, W. Andrews, A. Annan, B. Knoll, G. Tear and L. Bannister (2004). "Dynamic expression patterns of Robo (Robo1 and Robo2) in the developing murine central nervous system." J Comp Neurol 468(4): 467-81.

Trowe, T., S. Klostermann, H. Baier, M. Granato, A. D. Crawford, B. Grunewald, H. Hoffmann, R. O. Karlstrom, S. U. Meyer, B. Muller, S. Richter, C. Nusslein-Volhard and F. Bonhoeffer (1996). "Mutations disrupting the ordering and topographic mapping of axons in the retinotectal projection of the zebrafish, Danio rerio." Development 123: 439-50.

Walker, C. and G. Streisinger (1983). "Induction of Mutations by gamma-Rays in Pregonial Germ Cells of Zebrafish Embryos." Genetics 103(1): 125-136.

Wilson, S. W., L. S. Ross, T. Parrett and S. S. Easter, Jr. (1990). "The development of a simple scaffold of axon tracts in the brain of the embryonic zebrafish, Brachydanio rerio." Development 108(1): 121-45.

Xiao, T., T. Roeser, W. Staub and H. Baier (2005). "A GFP-based genetic screen reveals mutations that disrupt the architecture of the zebrafish retinotectal projection." Development 132(13): 2955-67.

Yook, K. J., S. R. Proulx and E. M. Jorgensen (2001). "Rules of nonallelic noncomplementation at the synapse in Caenorhabditis elegans." Genetics 158(1): 209-20.

Zallen, J. A., B. A. Yi and C. I. Bargmann (1998). "The conserved immunoglobulin superfamily member SAX-3/Robo directs multiple aspects of axon guidance in C. elegans." Cell 92(2): 217-27.

CHAPTER 4

DISCUSSION

Abstract

Slit and Robo define one of the canonical families of axon guidance ligands and receptors. They were originally characterized in the *Drosophila* ventral nerve cord and much of what is known about their signaling comes from this work. Slit-Robo signaling is also important in development of the vertebrate visual system, although it is less well understood. To expand our knowledge, I undertook in vitro experiments to confirm that Slit acts to collapse zebrafish RGC growth cones and that this collapse is mediated by the Robo2 receptor. I have also performed a forward genetic screen that was designed to isolate mutants that failed to complement Robo2 in zebrafish. Although this screen did not identify any mutations in new genes, it was successful in obtaining several new alleles of Robo2. These alleles have been characterized for phenotypic strength and sequenced to determine the molecular nature of their mutation. In this chapter, I discuss what the results teach us about Slit-Robo signaling.

Discussion

In Vitro Collapse Assays

Slit Causes Collapse in RGCs Mediated by Robo2

Slits have been known to acts as repellents both in *Drosophila* (Rothberg et al., 1988, 1990; Kidd et al., 1998a,b) and in vertebrates (Erskine et al., 2000; Niclou et al., 2000; Ringstedt et al., 2000). Although it is well established that Slits can act as repellents, it has not been formally confirmed that Slit acts through Robo receptors in vertebrates. This is an important distinction to make due to the differences between the

vertebrate visual system and the Drosophila ventral nerve cord, from where much of our knowledge comes.

The *astray* mutant makes zebrafish an optimal system to test for the requirement of the Robo2 receptor in Slit induced collapse of RGC growth cones (Fricke et al., 2001). First, however, I needed to confirm that Slits are repulsive for zebrafish RGCs, similar to the other vertebrate experiments in vitro. I have performed two sets of in vitro experiments to confirm Slits collapsing ability. The first one was using human Slit2 in conditioned media from a stably transfected cell line (gift from Y. Rao). The second approach used zebrafish Slit2 that was concentrated from the media of transient transfected cells. Both of these experiments clearly demonstrate that Slit2 (human or zebrafish) induces collapse in zebrafish RGC growth cones (Figure 2.4). This collapse was found to be dose-dependent, with higher amounts of Slit2 leading to a greater percentage of growth cones collapsing. Since the first round of experiments was imaged using fixed explants, I also performed a timecourse of the Slit2 induced collapse. This showed that strong collapse is evident as soon as 10 minutes after exposure to Slit2 (Fig 2.3).

Having confirmed that Slit acts to collapse RGCs, the next step was to see if the Robo2 receptor was required. In the zebrafish visual system, Robo2 is the only Robo family member expressed (Lee et al., 2001) so *astray* ^{ti272z} mutants (*ti272z* being a known null allele) have a complete removal of Robo signaling (Fricke et al., 2001). By performing collapse assays using Slit2 on explants derived from *astray* embryos, I demonstrated that the Robo2 receptor is required for Slit induced collapse (Figure 2.3).

This was true for both the *ti272z* and *te284* alleles. This is the first direct evidence that Slit acts through Robo in vertebrates, as in *Drosophila*.

Difficulties with In Vitro Approach

Zebrafish are an ideal choice for studying genetics (particularly in early development) but they have not been developed as a culture system. The necessity of confirming the requirement of Robo2 for Slit signaling and the existence of the zebrafish *astray* mutant led us to develop a protocol for explanting RGCs in culture. This development was not trivial and even after much trial and error, the axonal growth from these explants is not as robust as that seen from more established neuronal culture systems.

The other experimental issue was that I could not obtain reliable Slit1a protein and so was unable to test its effects in vitro. This was disappointing since evidence from our lab indicates that Slit1a is not acting as a simple repellent in the zebrafish visual system (Hardy and Chien, unpublished results). In trying to produce Slit1a protein, we made several different constructs using different promoters and tagging with GFP at either the N or C terminal. The problem was not one of expression as the cultured cells expressed GFP, which also confirmed that the constructs were good. The Slit1a-GFP transfections were always performed alongside Slit2-GFP and GFP only transfections for positive and negative controls. Although the Slit1a-transfected cells expressed GFP brightly, I had difficulty detecting it by Western blot using an anti-GFP antibody, even when the Slit2-GFP and GFP only samples were easily detected. Loading maximal amounts of sample sometimes, but not always, resulted in a faint band (Figure 2.5).

Noncomplementation Screen

Even with some difficulties with the culture approach, it has revealed that Slit2 acts through the Robo2 receptor in the zebrafish visual system. Having confirmed the ligand for Robo2, we then began to look at the receptor and how it might be signaling to elicit the changes in cytoskeletal dynamics that ultimately lead to growth cone guidance.

To our knowledge, this screen represents the largest forward genetic screen carried out in any vertebrate, screening 21,649 haploid genomes (Table 3.2). This should be enough coverage to recover mutations in other genes. So why was the screen successful in only identifying alleles of *astray*? There are several possibilities. The first is that even though several genes show a genetic interaction with Robo in *Drosophila*, they do not in vertebrates. To test this one would need to have a zebrafish mutation in one of the known interacting genes to generate embryos that are doubly heterozygous and see if they show a mutant phenotype; no such mutants yet exist. Of course, one of the merits of a forward genetic screen is the possibility of finding new genes that were previously unknown to interact.

Two other possibilities are that there are genes that do interact genetically with *astray*, but the interaction is incompletely penetrant or requires a mutation in a specific domain of the gene to elicit a mutant phenotype. Screening over 20,000 haploid genomes should be sufficient to recover muations in these types of genes unless the rarity becomes extreme.

One caveat is the difficulty in raising individual fry during the first half of the screen. Even though we screened 21,649 genomes, only mutants from the second half were successfully raised, meaning that effectively many of these genomes were

uninformative. Therefore, it is possible that the screen could have identified a mutant in a new gene in the first half but I was unable to successfully raise and breed it. However, the presence of mutants from the second half of the screen, all of which are allelic with *astray*, indicates that if there are interacting genes, they are few.

New *astray* Alleles

The screen recovered nine new alleles of *astray*. The new alleles that are missense mutations all represent conserved residues, suggesting that these residues are important for proper Robo signaling. Interestingly, they all represent mutations in the extracellular portion of the receptor. Combined with the alleles from the original Tübingen screen (Karlstrom et al., 1996; Trowe et al., 1996), we now have many alleles but no mutations in the intracellular domain (although *te284* is a mutation in the transmembrane domain). Although it is formally possible that we have simply been unfortunate in only obtaining extracellular mutants (the intracellular domain represents 41% of the receptor), it seems much more likely that intracellular mutants are less likely to demonstrate a phenotype. The intracellular region of the receptor is less conserved with other Robo family members compared to the extracellular region (Simpson et al., 2000). There may be few intracellular residues that provide a suitable target for missense mutations, though it is still expected that an introduced stop codon that removed many or all of the CC domains would be a null and have a strong phenotype.

The eight-point scoring of phenotypic strength is useful in establishing an allelic series for the *astray* gene. It shows that other alleles are weaker than *te284*, and confirms the null phenotype of several alleles. In addition, the observation of the ‘one tecta’

phenotype is a new observation that had not previously been identified in any of the four previous *astray* alleles. This striking phenotype, made only by two of the weak alleles, is generated by retino-retinal pathfinding errors. Although the null allele *ti272z* is known to cause some axons to make these types of mistakes, it is unusual for all the axons of an entire eye to make them together and exclusively.

Future Directions

In Vitro Assays

The development of explanting zebrafish RGCs in culture is a useful tool that could likely still reveal more about Slit Robo signaling. In addition to collapse, more subtle effects such as changes in growth rates or neurite branching could be observed. The requirement of the Astray receptor has been demonstrated by using the *te284* and *ti272z* alleles. It would be interesting to test if some of the weaker *astray* alleles showed intermediate collapse in response to Slit. And of course, it would be interesting to test the effects of other zebrafish Slits, particularly Slit1a.

The collapse assays could be expanded to test for requirements of candidate signaling molecules in same manner that *astray* was tested. Since we do not have existing mutants in these genes, we could use morpholinos to reduce gene function and generate explants. This could be a very informative approach to see if signaling is conserved between vertebrates and *Drosophila*.

Screening for Robo Signaling Mutants

Although the current screen was unsuccessful in revealing nonallelic noncomplementation, it may be possible to design a new screen that would identify mutants. One possible approach would be to use one of the newly generated weak alleles, such as *zc10*, to perform a suppressor screen. This allele is fully penetrant, although it generally makes few mistakes (Figure 3.3). One could mutagenize *zc10* homozygotes and screen for wildtype embryos. Another possibility would be a F2 enhancer screen, but this would be more laborious in that many embryos would need to be scored for each mutagenized haploid genome.

References

Erskine, L., S. E. Williams, K. Brose, T. Kidd, R. A. Rachel, C. S. Goodman, M. Tessier-Lavigne and C. A. Mason (2000). "Retinal ganglion cell axon guidance in the mouse optic chiasm: expression and function of robos and slits." J Neurosci 20(13): 4975-82.

Fricke, C., J. S. Lee, S. Geiger-Rudolph, F. Bonhoeffer and C. B. Chien (2001). "astray, a zebrafish roundabout homolog required for retinal axon guidance." Science 292(5516): 507-10.

Karlstrom, R. O., T. Trowe, S. Klostermann, H. Baier, M. Brand, A. D. Crawford, B. Grunewald, P. Haffter, H. Hoffmann, S. U. Meyer, B. K. Muller, S. Richter, F. J. van Eeden, C. Nusslein-Volhard and F. Bonhoeffer (1996). "Zebrafish mutations affecting retinotectal axon pathfinding." Development 123: 427-38.

Kidd, T., C. Russell, C. S. Goodman and G. Tear (1998a). "Dosage-sensitive and complementary functions of roundabout and commissureless control axon crossing of the CNS midline." Neuron 20(1): 25-33.

Kidd, T., K. Brose, K. J. Mitchell, R. D. Fetter, M. Tessier-Lavigne, C. S. Goodman and G. Tear (1998b). "Roundabout controls axon crossing of the CNS midline and defines a novel subfamily of evolutionarily conserved guidance receptors." Cell 92(2): 205-15.

Lee, J. S., R. Ray and C. B. Chien (2001). "Cloning and expression of three zebrafish roundabout homologs suggest roles in axon guidance and cell migration." Dev Dyn 221(2): 216-30.

Niclou, S. P., L. Jia and J. A. Raper (2000). "Slit2 is a repellent for retinal ganglion cell axons." J Neurosci 20(13): 4962-74.

Ringstedt, T., J. E. Braisted, K. Brose, T. Kidd, C. Goodman, M. Tessier-Lavigne and D. D. O'Leary (2000). "Slit inhibition of retinal axon growth and its role in retinal axon pathfinding and innervation patterns in the diencephalon." J Neurosci 20(13): 4983-91.

Rothberg, J. M., D. A. Hartley, Z. Walther and S. Artavanis-Tsakonas (1988). "slit: an EGF-homologous locus of D. melanogaster involved in the development of the embryonic central nervous system." Cell 55(6): 1047-59.

Rothberg, J. M., J. R. Jacobs, C. S. Goodman and S. Artavanis-Tsakonas (1990). "slit: an extracellular protein necessary for development of midline glia and commissural axon pathways contains both EGF and LRR domains." Genes Dev 4(12A): 2169-87.

Simpson, J. H., T. Kidd, K. S. Bland and C. S. Goodman (2000). "Short-range and long-range guidance by slit and its Robo receptors. Robo and Robo2 play distinct roles in midline guidance." Neuron 28(3): 753-66.

Trowe, T., S. Klostermann, H. Baier, M. Granato, A. D. Crawford, B. Grunewald, H. Hoffmann, R. O. Karlstrom, S. U. Meyer, B. Muller, S. Richter, C. Nusslein-Volhard and F. Bonhoeffer (1996). "Mutations disrupting the ordering and topographic mapping of axons in the retinotectal projection of the zebrafish, Danio rerio." Development 123: 439-50.